



Australian
National
University



Ultra-light dark matter searches with gravitational wave detectors

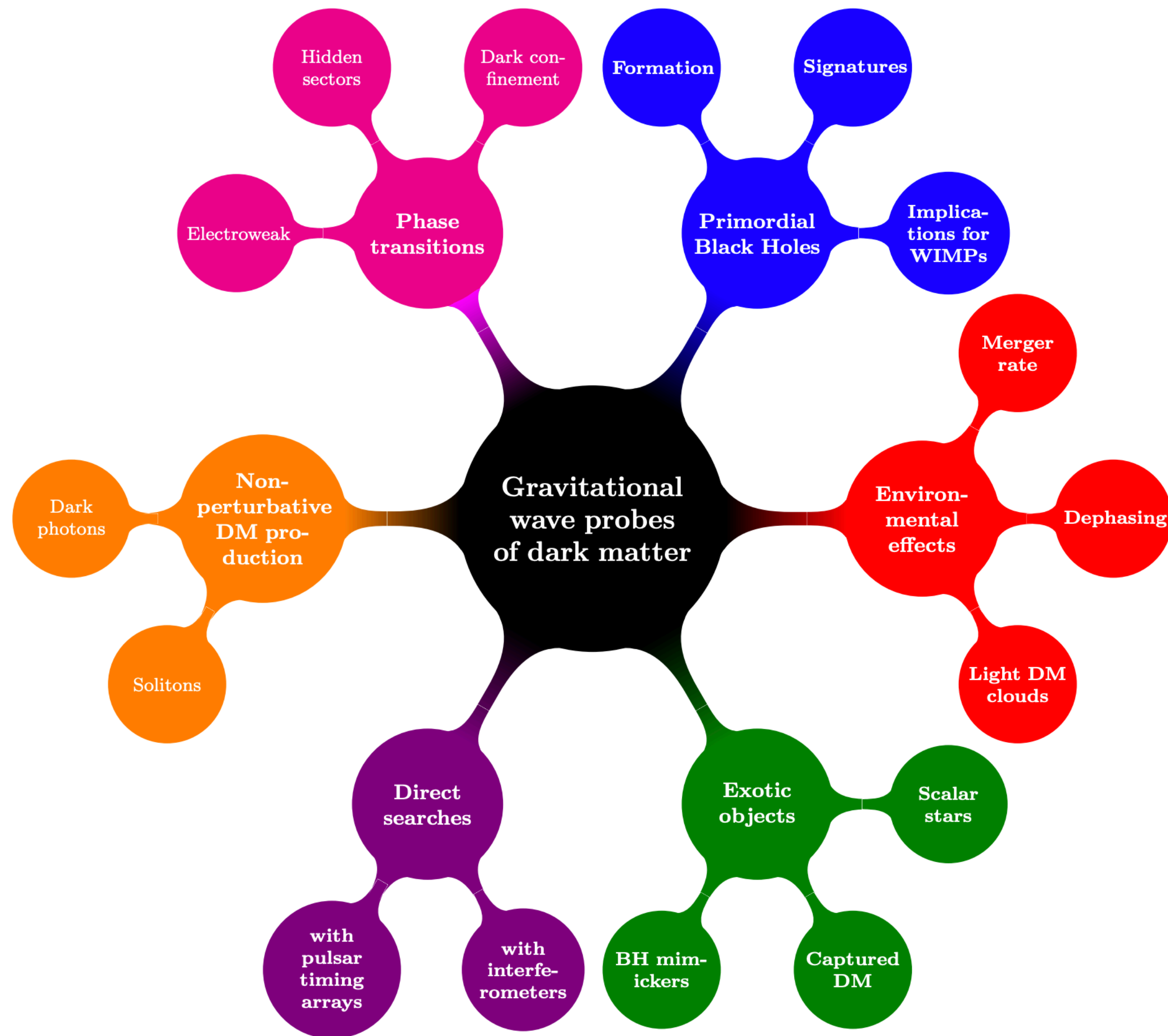
30 Years of Gravity Research in Australasia: Past Reflections and Future Ambitions
Canberra, Australia

Ornella J. Piccinni

2 September 2024

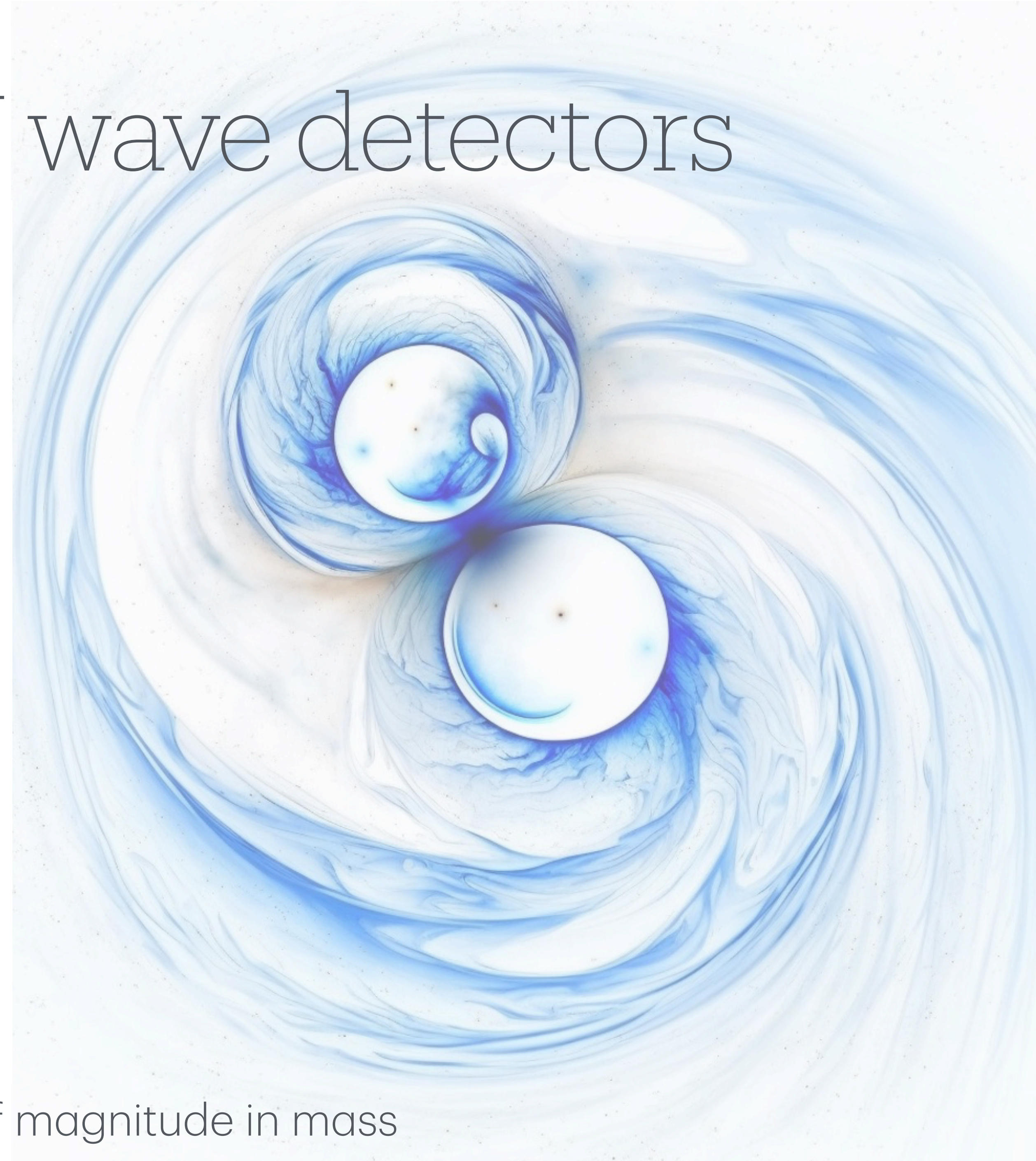
ARC Centre of Excellence for Gravitational Wave Discovery (OzGrav) and
Centre for Gravitational Astrophysics,
The Australian National University, Canberra, Australia

Dark matter and GW wave detectors

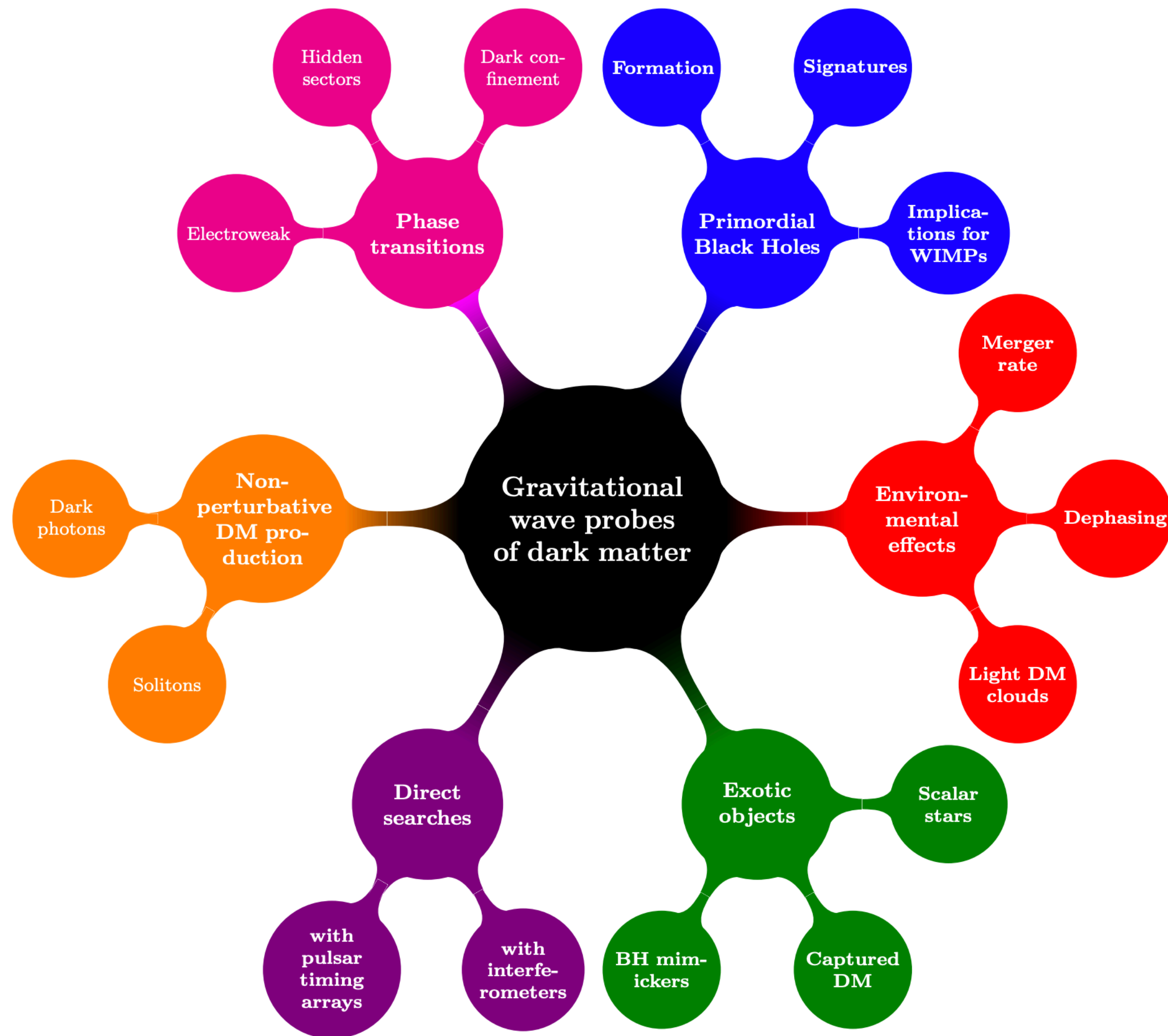


Credit: Bertone et al. 2020

~90 orders of magnitude in mass



Dark matter and GW wave detectors



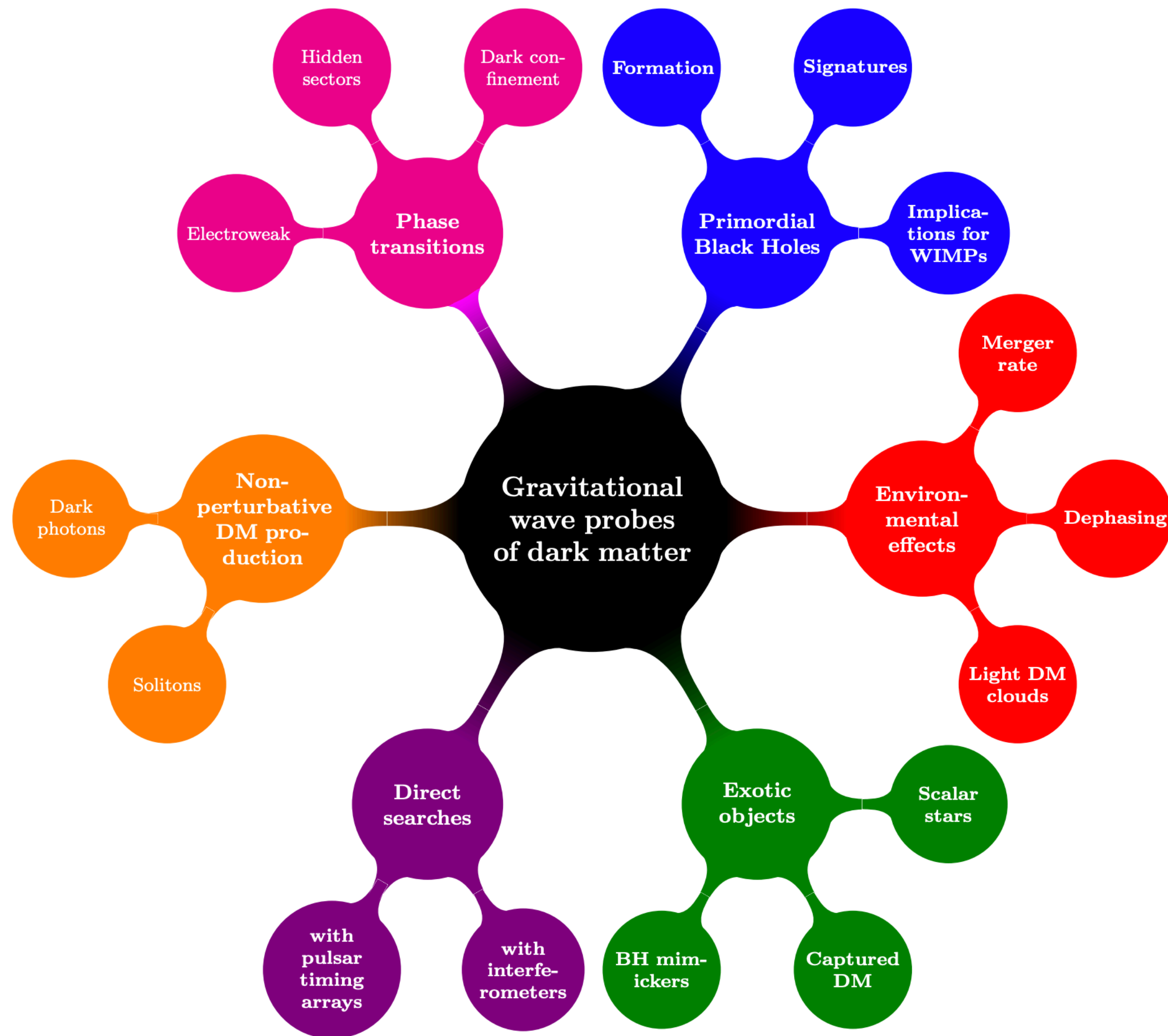
Credit: Bertone et al. 2020

~90 orders of magnitude in mass

Direct interaction of particles with the detector

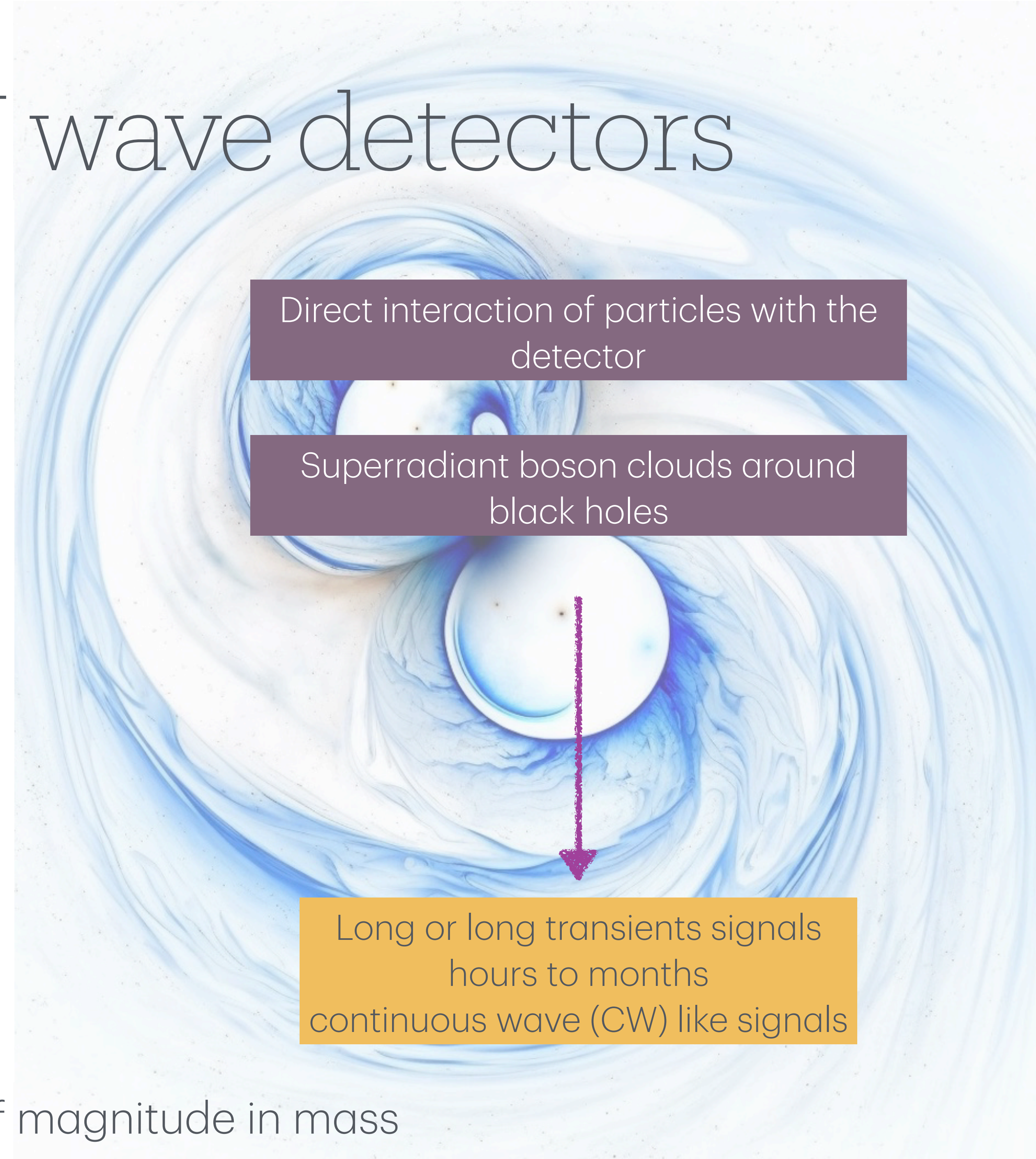
Superradiant boson clouds around black holes

Dark matter and GW wave detectors



Credit: Bertone et al. 2020

~90 orders of magnitude in mass



Ultralight particles interacting
with the detector

Direct interaction with the detectors

ULDM of spin-0 (scalar), 1 (vector), or 2 (tensors) interacting with the detector optics (mirrors)

Direct interaction with the detectors

ULDM of spin-0 (scalar), 1 (vector), or 2 (tensors) interacting with the detector optics (mirrors)

Scalars

space-time variation of
fundamental constants (fine
structure constant or the proton-
electron mass ratio)
+
Finite light travel time

Direct interaction with the detectors

ULDM of spin-0 (scalar), 1 (vector), or 2 (tensors) interacting with the detector optics (mirrors)

Scalars

space-time variation of
fundamental constants (fine
structure constant or the proton-
electron mass ratio)
+
Finite light travel time

Vectors

$U(1)_B$ or $U(1)_{B-L}$ bosons
spatial gradient of the dark
photon field
+
Finite light travel time

Direct interaction with the detectors

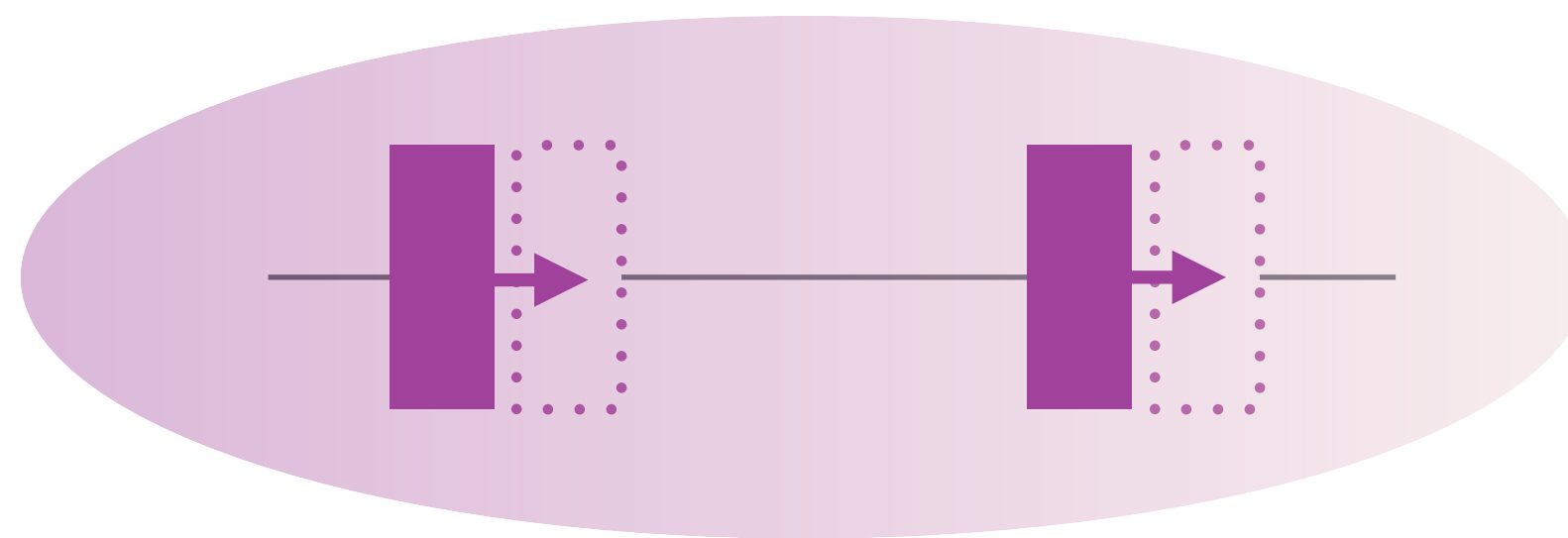
ULDM of spin-0 (scalar), 1 (vector), or 2 (tensors) interacting with the detector optics (mirrors)

Scalars

space-time variation of
fundamental constants (fine
structure constant or the proton-
electron mass ratio)
+
Finite light travel time

Vectors

$U(1)_B$ or $U(1)_{B-L}$ bosons
spatial gradient of the dark
photon field
+
Finite light travel time



Arvanitaki et al., PRD 91, 015015 (2015)
Stadnik and Flambaum, PRA 93, 063630 (2016)
Morisaki et al., PRD 100, 123512 (2019)
Vermulen et al., Nature, 600, pages 424–428 (2021)
Göttel et al., 2401.18076

Pierce et al., PRL 121, 061102 (2018)
Guo et al., Nat. Comm. Phys. 2, 155 (2019)
Morisaki et al., PRD 103, L051702 (2021)

Direct interaction with the detectors

ULDM of spin-0 (scalar), 1 (vector), or 2 (tensors) interacting with the detector optics (mirrors)

Scalars

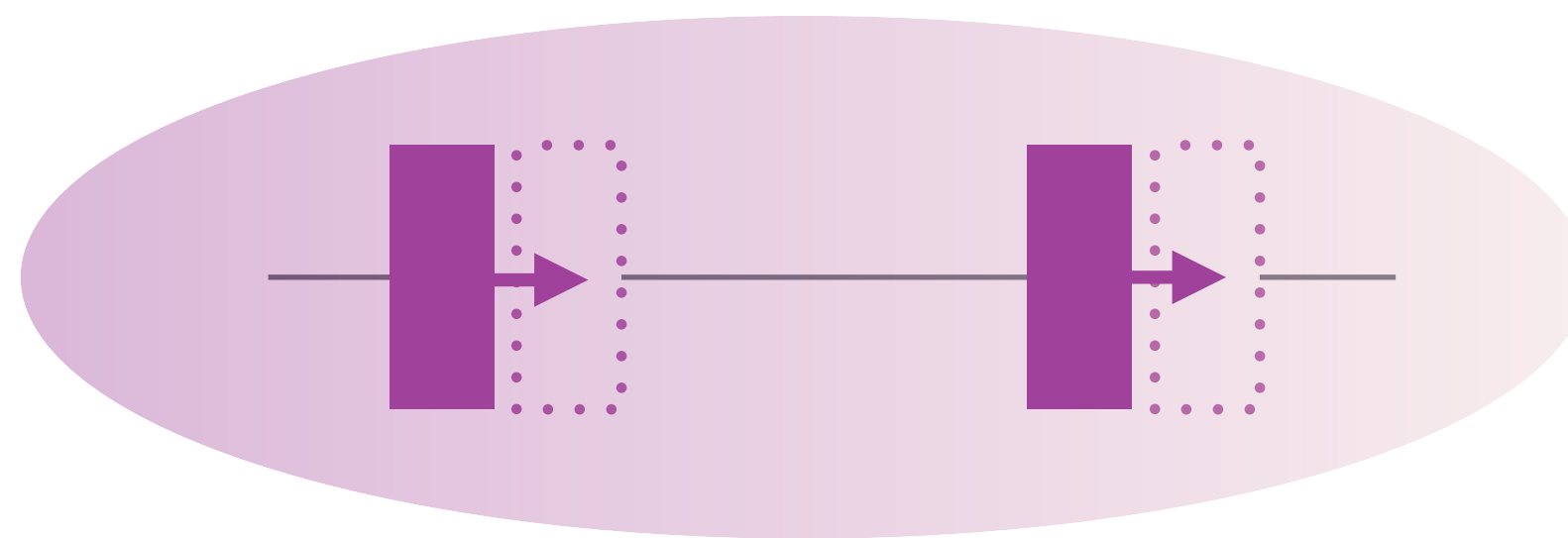
space-time variation of
fundamental constants (fine
structure constant or the proton-
electron mass ratio)
+
Finite light travel time

Vectors

$U(1)_B$ or $U(1)_{B-L}$ bosons
spatial gradient of the dark
photon field
+
Finite light travel time

Tensors

Coupling with energy-
momentum tensors of SM
(same mechanism of GWs)



Arvanitaki et al., PRD 91, 015015 (2015)
Stadnik and Flambaum, PRA 93, 063630 (2016)
Morisaki et al., PRD 100, 123512 (2019)
Vermulen et al., Nature, 600, pages 424–428 (2021)
Göttel et al., 2401.18076

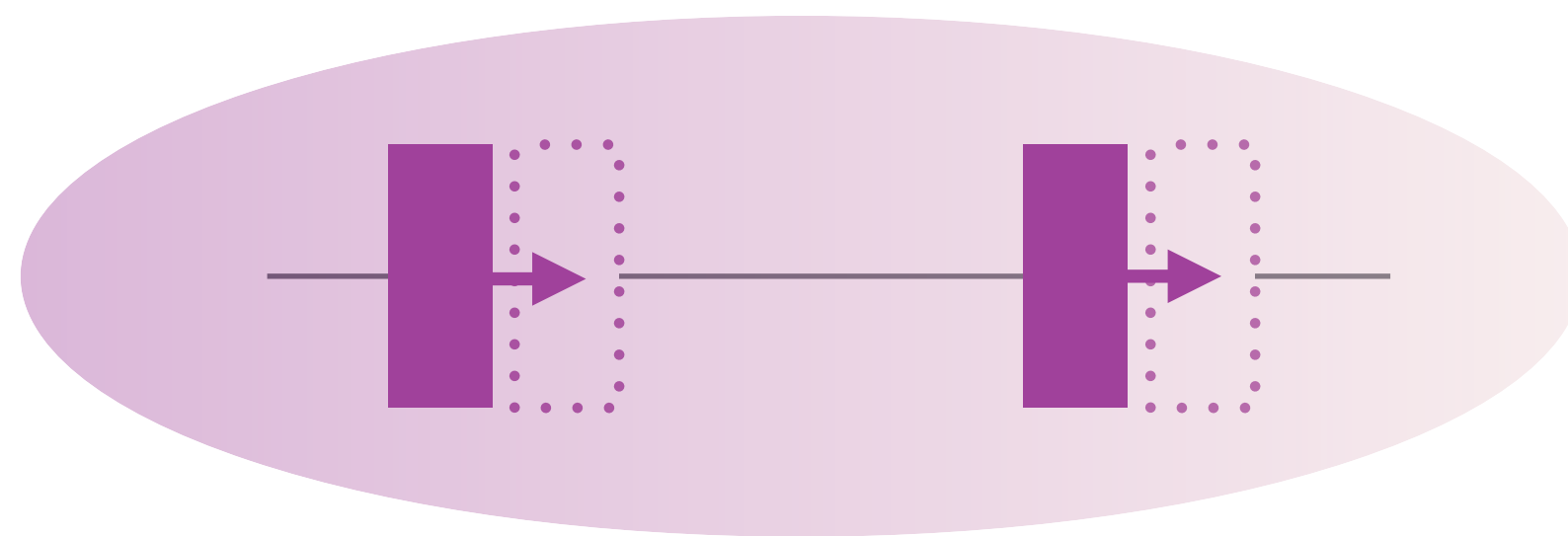
Pierce et al., PRL 121, 061102 (2018)
Guo et al., Nat. Comm. Phys. 2, 155 (2019)
Morisaki et al., PRD 103, L051702 (2021)

Direct interaction with the detectors

ULDM of spin-0 (scalar), 1 (vector), or 2 (tensors) interacting with the detector optics (mirrors)

Scalars

space-time variation of
fundamental constants (fine
structure constant or the proton-
electron mass ratio)
+
Finite light travel time



Arvanitaki et al., PRD 91, 015015 (2015)
Stadnik and Flambaum, PRA 93, 063630 (2016)
Morisaki et al., PRD 100, 123512 (2019)
Vermulen et al., Nature, 600, pages 424–428 (2021)
Göttel et al., 2401.18076

Vectors

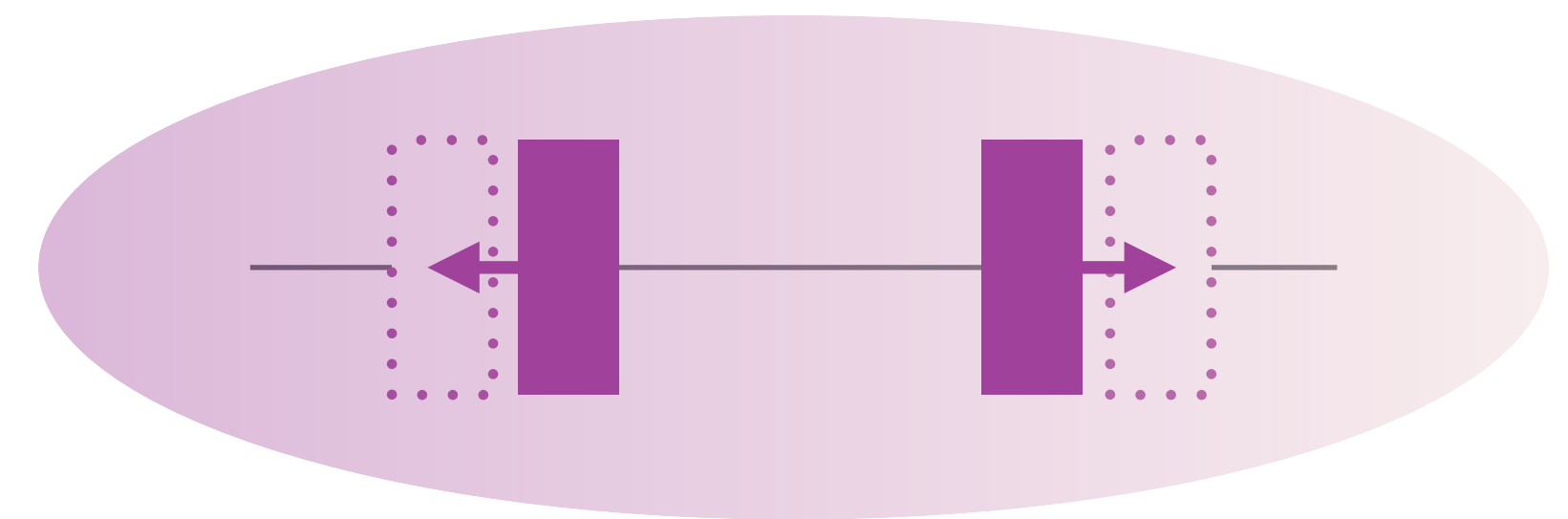
$U(1)_B$ or $U(1)_{B-L}$ bosons
spatial gradient of the dark
photon field
+
Finite light travel time



Pierce et al., PRL 121, 061102 (2018)
Guo et al., Nat. Comm. Phys. 2, 155 (2019)
Morisaki et al., PRD 103, L051702 (2021)

Tensors

Coupling with energy-
momentum tensors of SM
(same mechanism of GWs)



Armaleo et al., JCAP04(2021)053
Manita et al., PRD 107, 104007 (2023)

Vector bosons (dark photons) strain

LVK, Abbott et al., PRD 105, 063030, 2022; Guo et al., Comm. Phys 2, 155 (2019)

Vector bosons (dark photons) strain

LVK, Abbott et al., PRD 105, 063030, 2022; Guo et al., Comm. Phys 2, 155 (2019)

- ULDM interacting with GW interferometers (baryons/baryons minus leptons in the materials - fused silica). *Treated as an oscillatory “classical field”*

Vector bosons (dark photons) strain

LVK, Abbott et al., PRD 105, 063030, 2022; Guo et al., Comm. Phys 2, 155 (2019)

- ULDM interacting with GW interferometers (baryons/baryons minus leptons in the materials - fused silica). *Treated as an oscillatory “classical field”*
- The differential strain due to:

Vector bosons (dark photons) strain

LVK, Abbott et al., PRD 105, 063030, 2022; Guo et al., Comm. Phys 2, 155 (2019)

- ULDM interacting with GW interferometers (baryons/baryons minus leptons in the materials - fused silica). *Treated as an oscillatory “classical field”*
- The differential strain due to:
 - A **spatial gradient** → relative acceleration between the objects due to the different field amplitude

$$\sqrt{\langle h_D^2 \rangle} = C \frac{q}{M} \frac{e\epsilon}{2\pi c^2} \sqrt{\frac{2\rho_{\text{DM}}}{\epsilon_0}} \frac{v_0}{f_0} = 6.28 \times 10^{-27} \left(\frac{\epsilon}{10^{-23}} \right) \left(\frac{100 \text{ Hz}}{f_0} \right)$$

Pierce et al. 2018, PRL 121, 061102

Vector bosons (dark photons) strain

LVK, Abbott et al., PRD 105, 063030, 2022; Guo et al., Comm. Phys 2, 155 (2019)

- ULDM interacting with GW interferometers (baryons/baryons minus leptons in the materials - fused silica). *Treated as an oscillatory “classical field”*
- The differential strain due to:
 - A **spatial gradient** → relative acceleration between the objects due to the different field amplitude

$$\sqrt{\langle h_D^2 \rangle} = C \frac{q}{M} \frac{e\epsilon}{2\pi c^2} \sqrt{\frac{2\rho_{\text{DM}}}{\epsilon_0}} \frac{v_0}{f_0} = 6.28 \times 10^{-27} \left(\frac{\epsilon}{10^{-23}} \right) \left(\frac{100 \text{ Hz}}{f_0} \right)$$

Pierce et al. 2018, PRL 121, 061102

- Effect due to the **finite light travel time**

$$\sqrt{\langle h_C^2 \rangle} = \frac{\sqrt{3}}{2} \sqrt{\langle h_D^2 \rangle} \left(\frac{2\pi f_0 L}{v_0} \right) \simeq 6.21 \times 10^{-26} \left(\frac{\epsilon}{10^{-23}} \right)$$

Morisaki et al. 2021, PRD 103, 051702

DM signal - CW like signal

DM signal - CW like signal

A time-dependent force acting on the test masses.
Oscillating at the same frequency and phase as the DM field
(superposition of plane waves)

$$\boxed{f_0 = m_A c^2 / (2\pi\hbar)} \longrightarrow \frac{\Delta f}{f_0} = \frac{1}{2} \frac{v_0^2}{c^2} \approx 2.94 \times 10^{-7} + \text{Doppler effect } (\sim 10^{-8})$$

Maxwell-Boltzmann spreading $\Delta f_e = \frac{1}{2\pi} \frac{v_0 v_E}{c^2} f_0 \approx 10^{-8} f_0.$

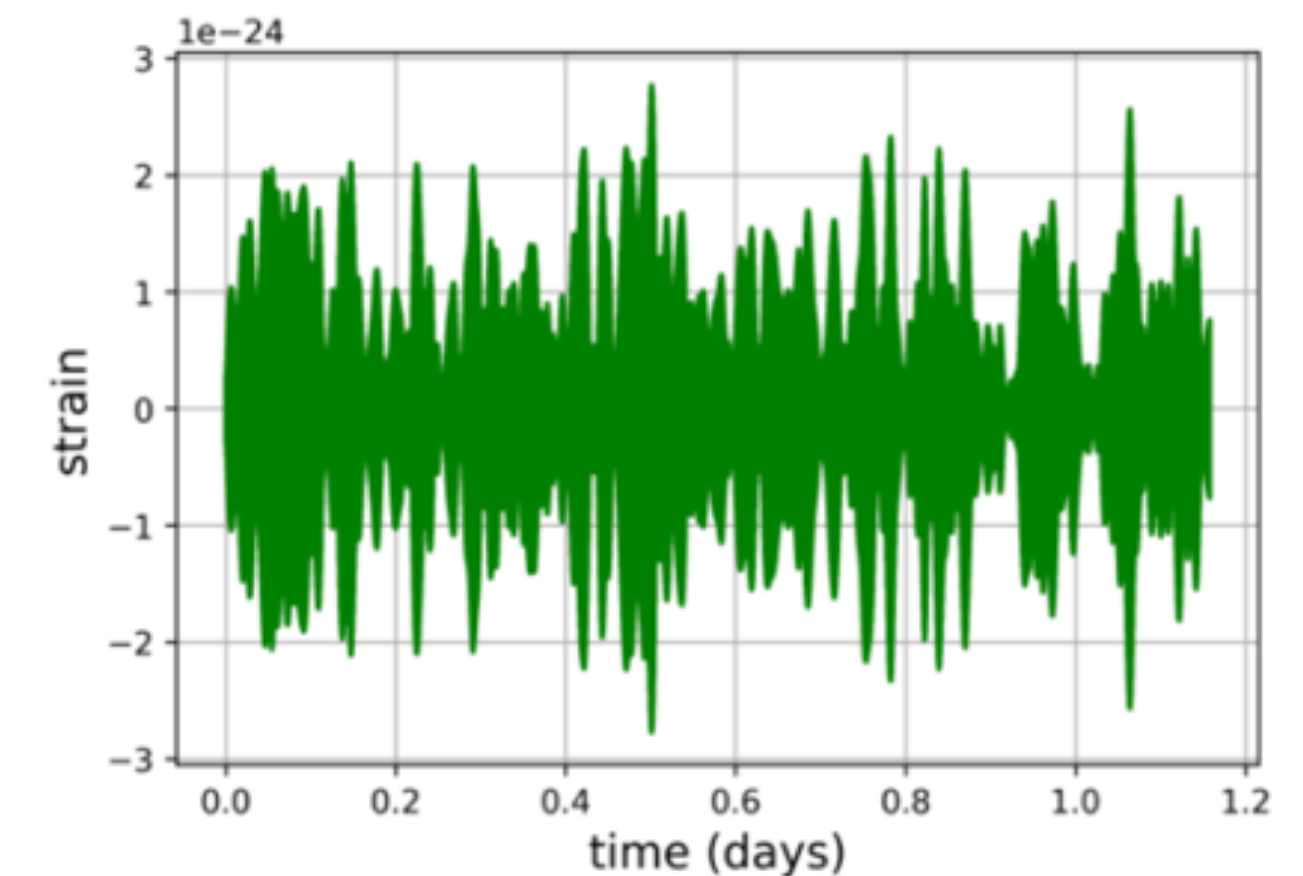
DM signal - CW like signal

A time-dependent force acting on the test masses.
Oscillating at the same frequency and phase as the DM field
(superposition of plane waves)

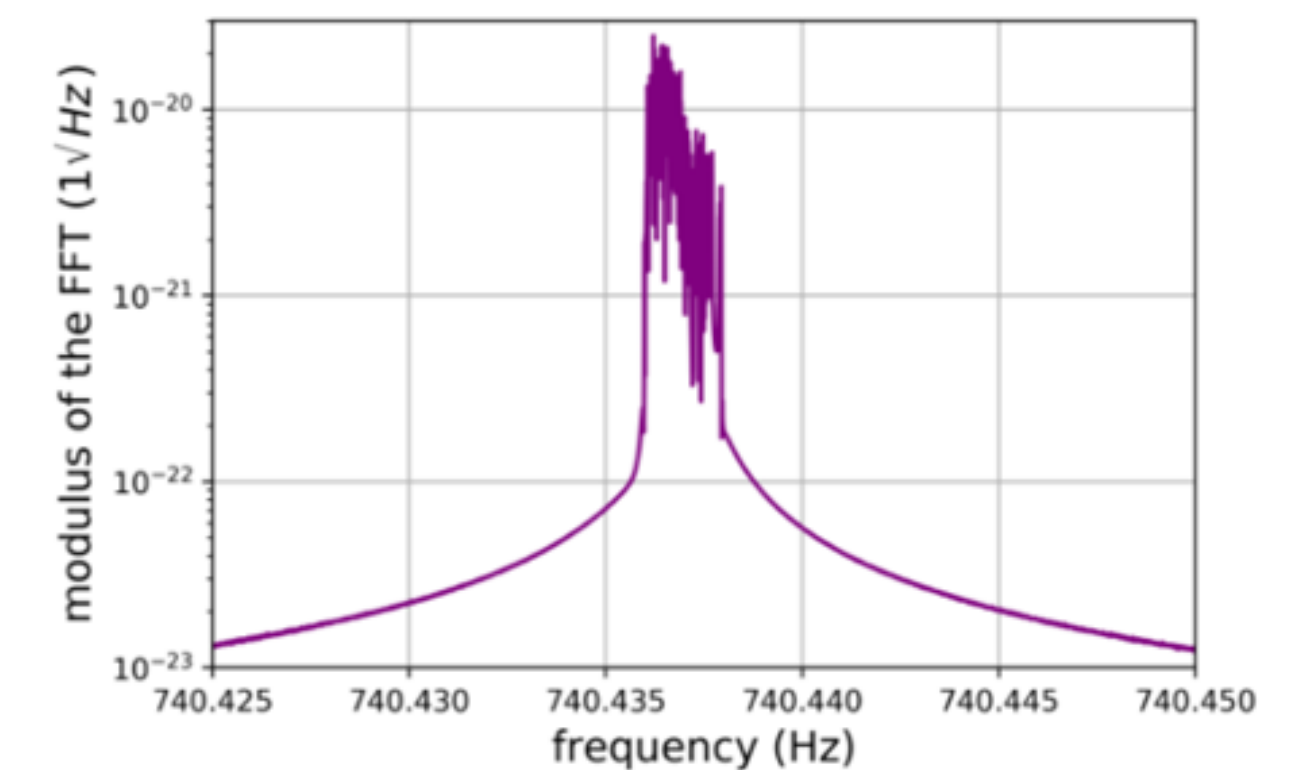
$$\boxed{f_0 = m_A c^2 / (2\pi \hbar)} \longrightarrow \frac{\Delta f}{f_0} = \frac{1}{2} \frac{v_0^2}{c^2} \approx 2.94 \times 10^{-7} \text{ + Doppler effect } (\sim 10^{-8})$$

Maxwell-Boltzmann spreading $\Delta f_e = \frac{1}{2\pi} \frac{v_0 v_E}{c^2} f_0 \approx 10^{-8} f_0.$

Stochastic and narrowband signal



(a)



(b)

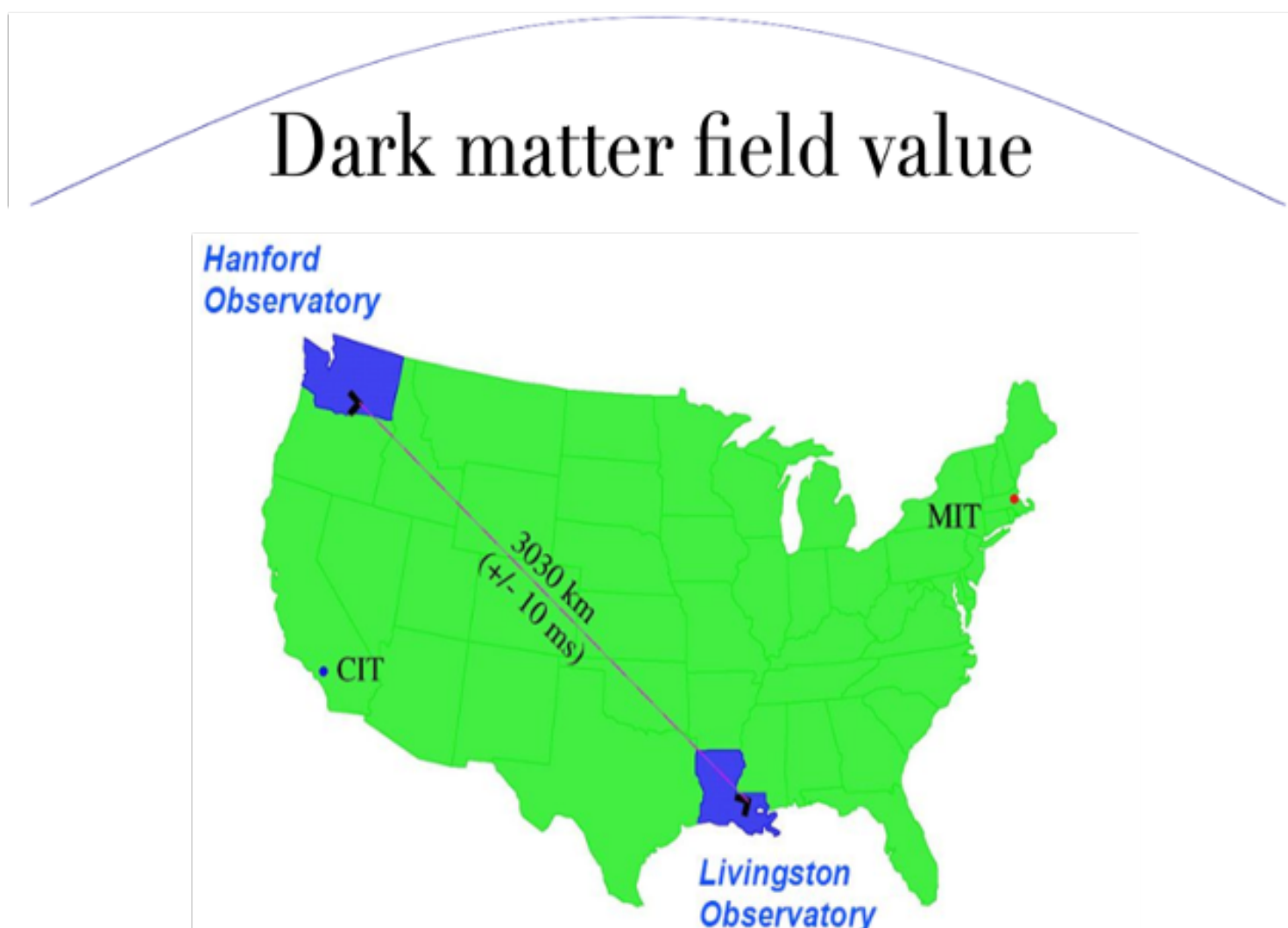
DM signal - CW like signal

A time-dependent force acting on the test masses.
Oscillating at the same frequency and phase as the DM field
(superposition of plane waves)

$$f_0 = m_A c^2 / (2\pi\hbar) \longrightarrow \frac{\Delta f}{f_0} = \frac{1}{2} \frac{v_0^2}{c^2} \approx 2.94 \times 10^{-7} + \text{Doppler effect } (\sim 10^{-8})$$

Maxwell-Boltzmann spreading $\Delta f_e = \frac{1}{2\pi} \frac{v_0 v_E}{c^2} f_0 \approx 10^{-8} f_0.$

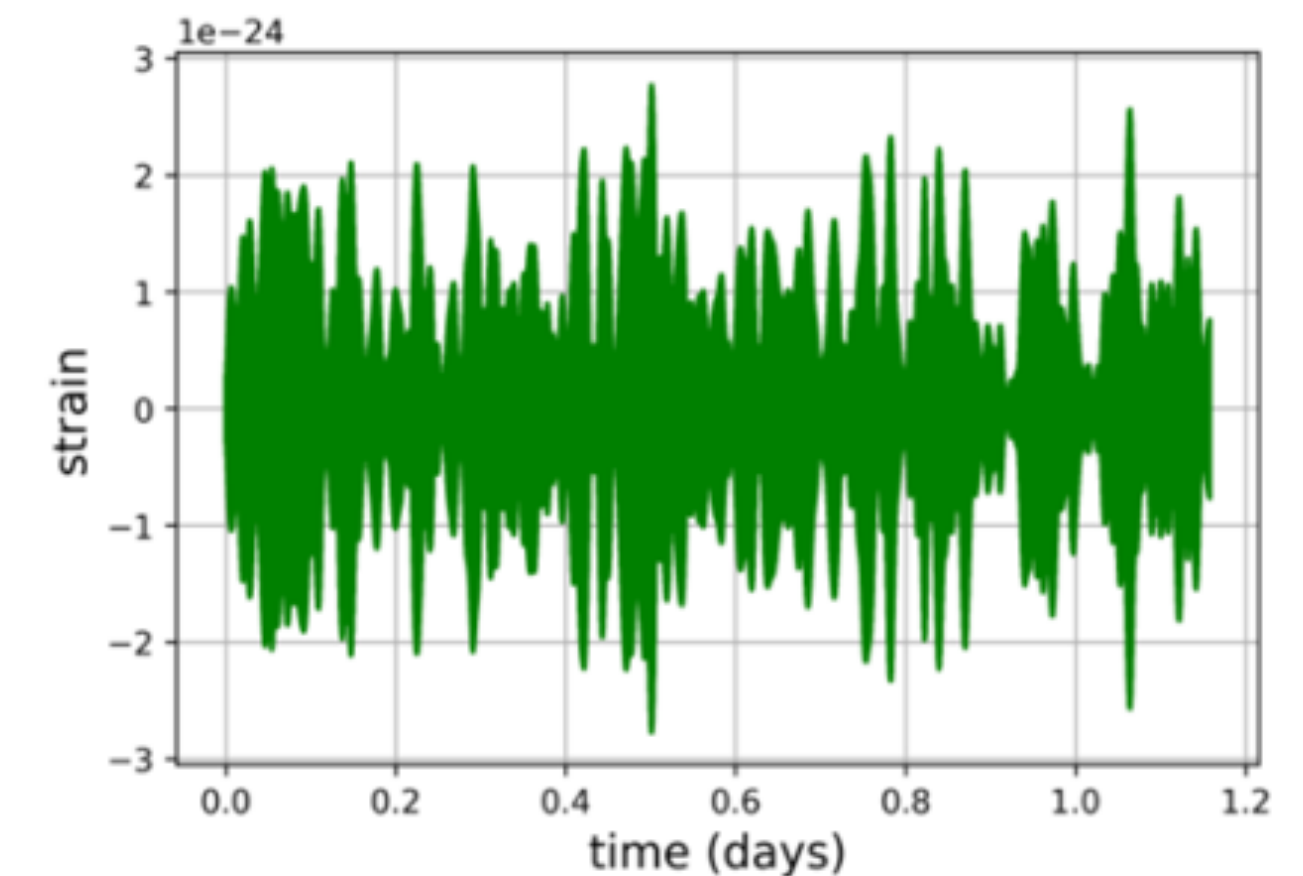
The coherence time \gg detectors separation



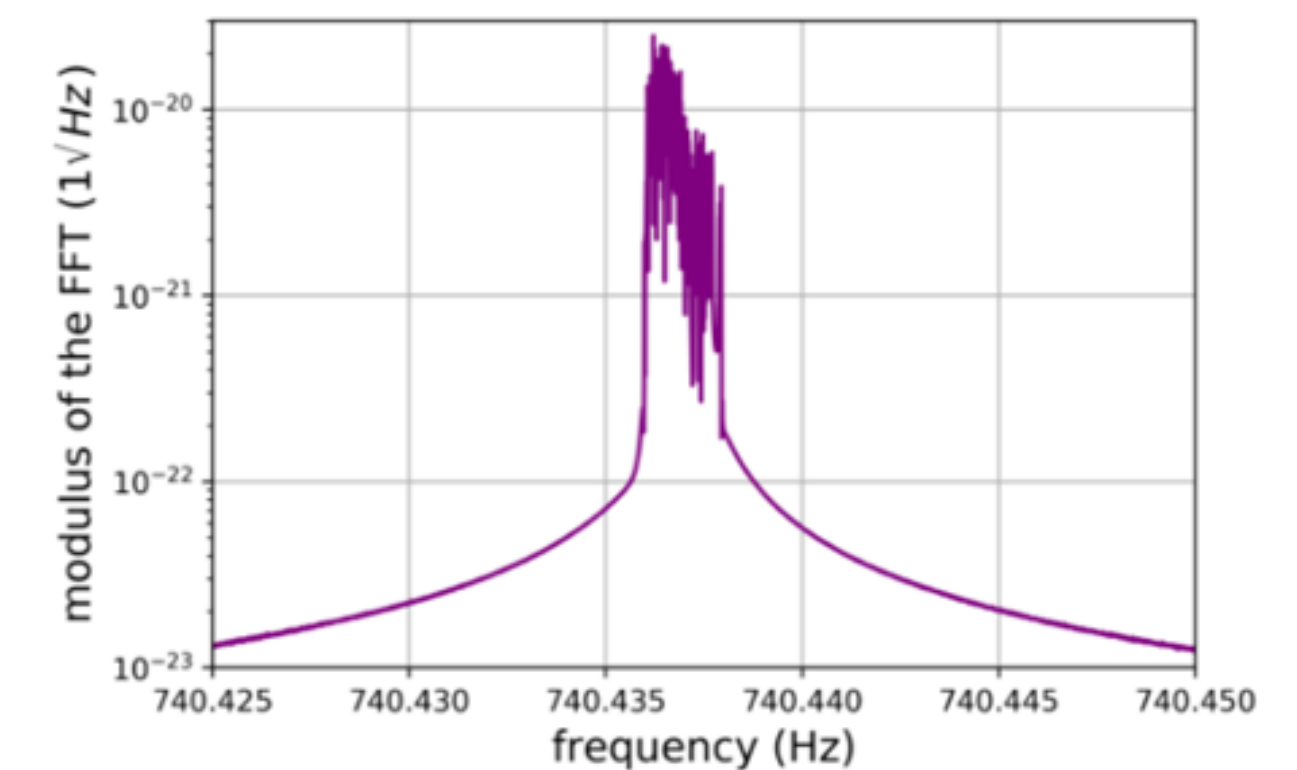
$$L_{\text{coh}} = \frac{2\pi\hbar}{m_A v_0} = 1.6 \times 10^9 \text{ m} \left(\frac{10^{-12} \text{ eV}/c^2}{m_A} \right)$$

We can look for coincidences
between detectors

Stochastic and narrowband signal



(a)



(b)

Search on O3 LIGO/Virgo data

Methods and results - LVK, Abbott et al., PRD 105, 063030, 2022

- **Cross-correlation** Pierce et al., PRL121, 061121 (2018)
- **Excess power (BSD)** Miller et al., PRD 103, 103002 (2021)

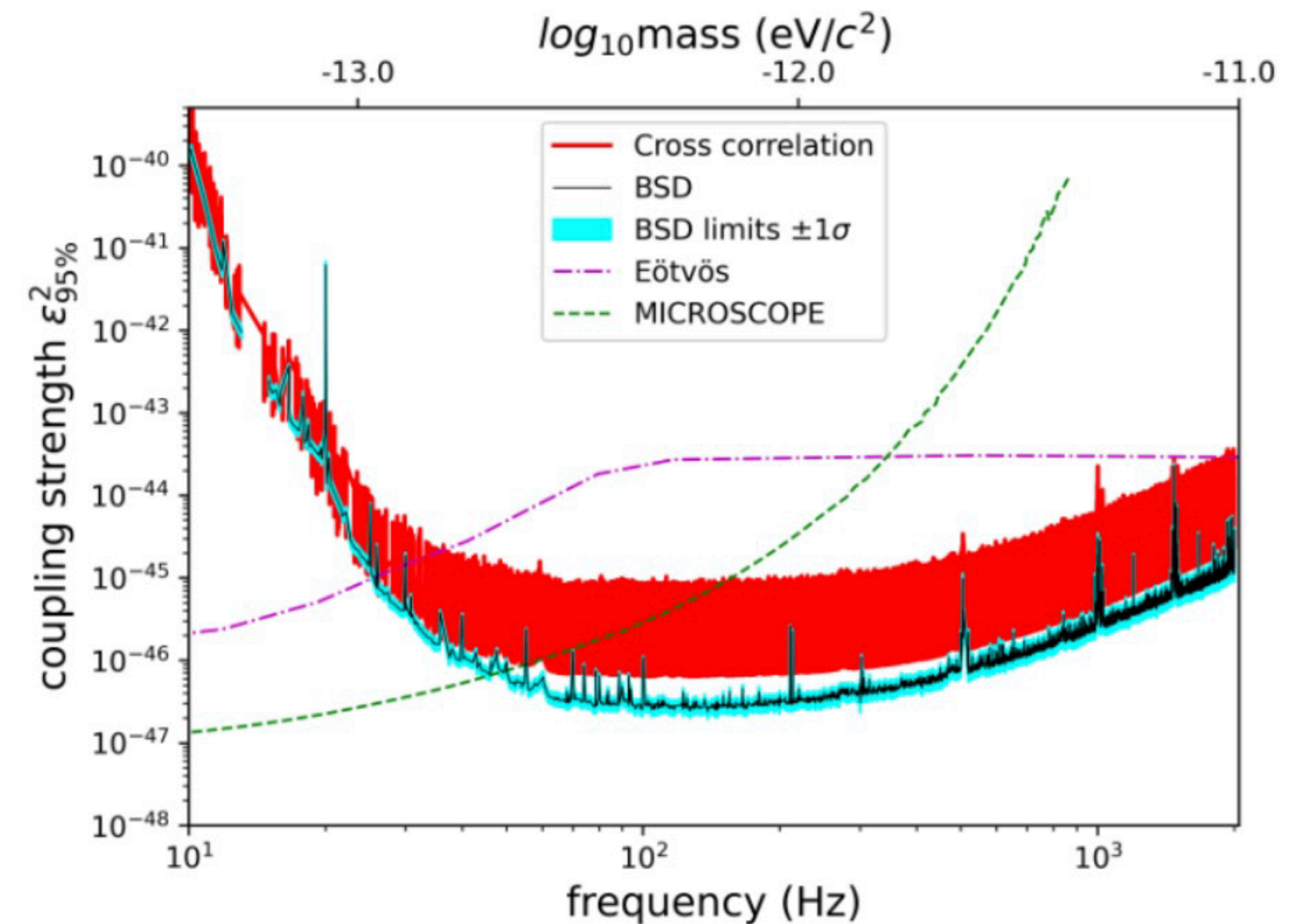
No detection → limits on coupling

$$\mathcal{L} = -\frac{\epsilon_0 c^2}{4} F^{\mu\nu} F_{\mu\nu} + \frac{\epsilon_0}{2} \left(\frac{m_A c^2}{\hbar} \right)^2 A^\mu A_\mu - \epsilon_D e J_D^\mu A_\mu,$$

m_A : dark photon mass

ϵ_D : coupling strength

A_μ : dark vector potential



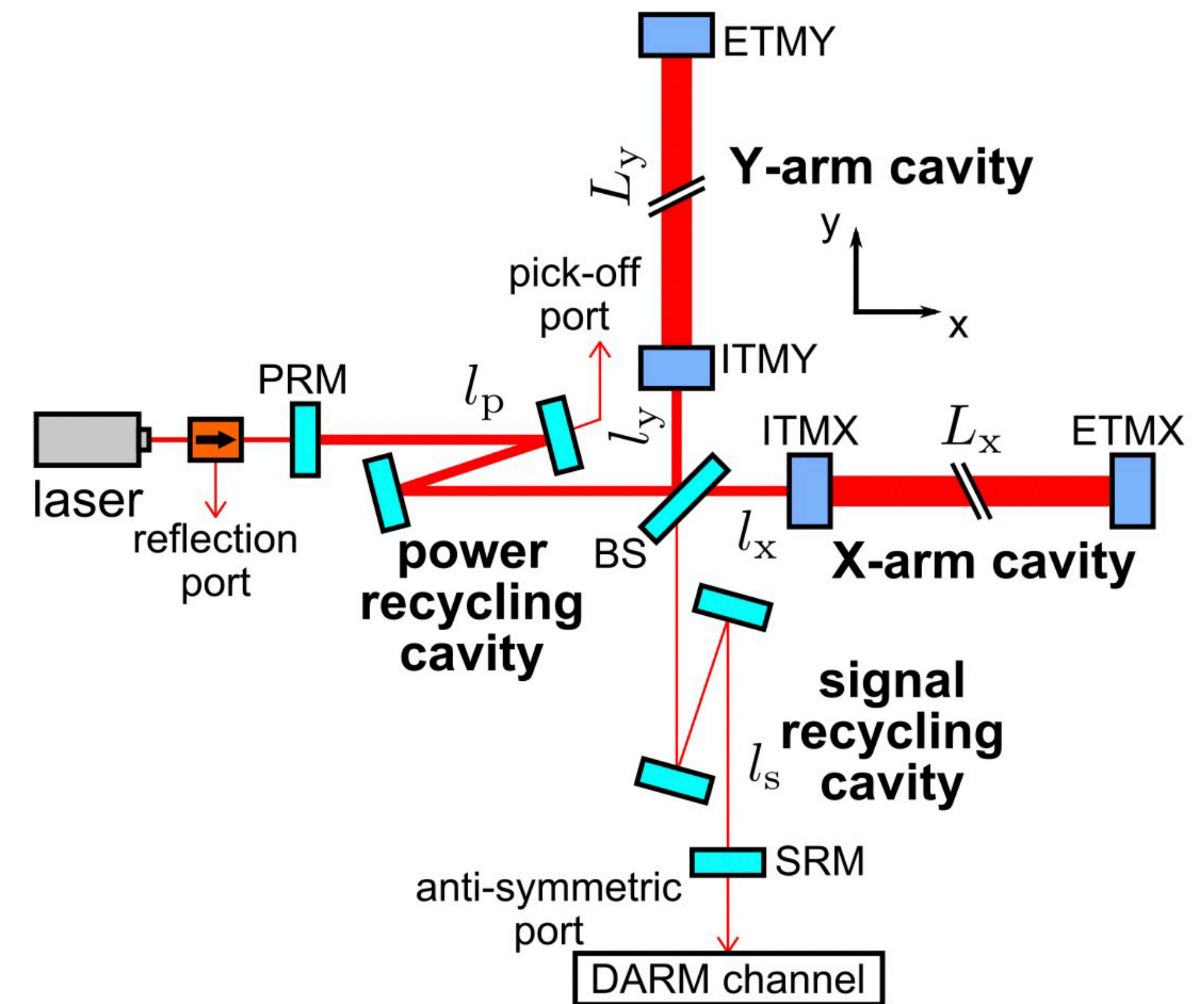
LVK PRD 105, 063030 (2022) updated in erratum <https://dcc.ligo.org/LIGO-P2300439/public>

Vector DM search in KAGRA

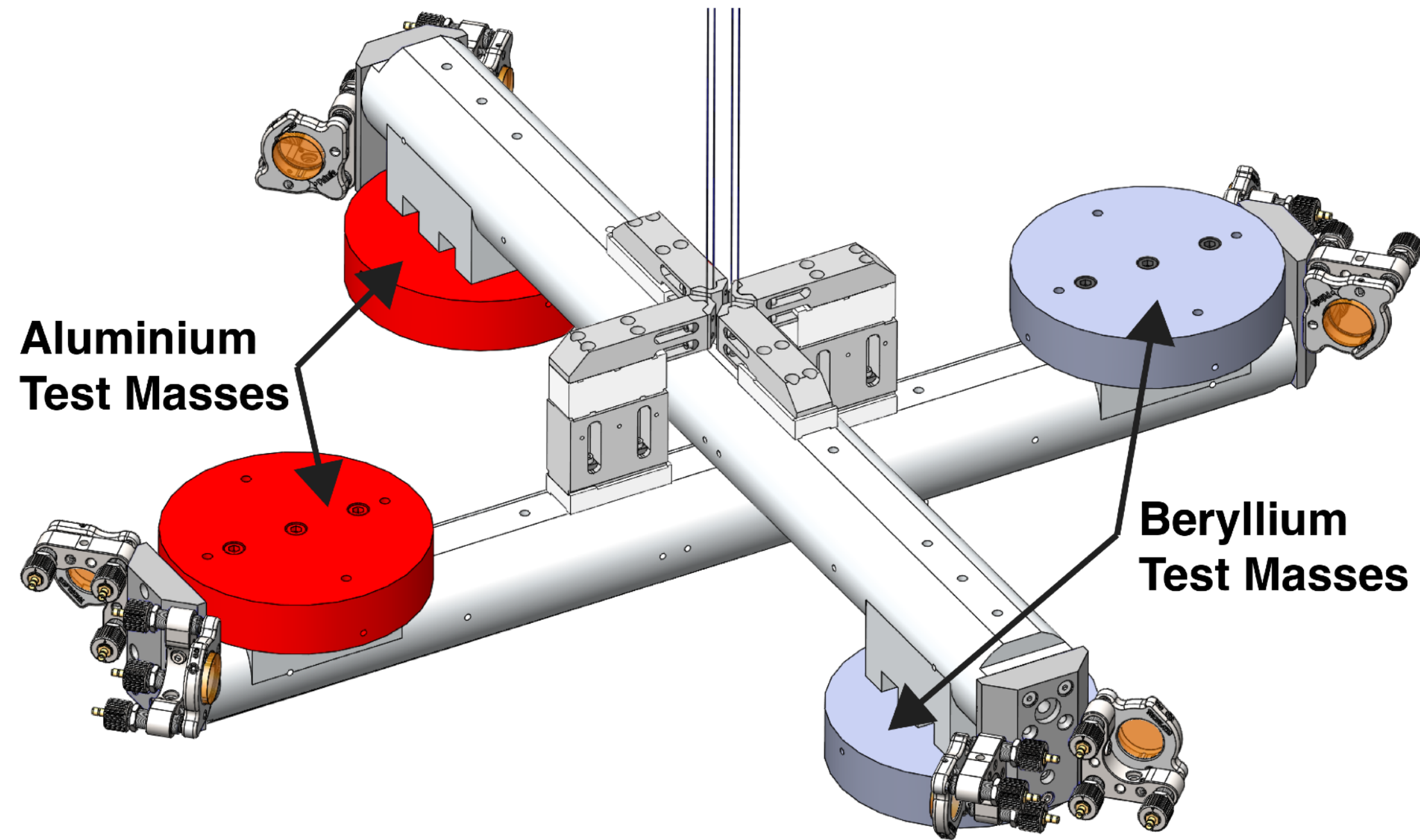
- **Vector fields in KAGRA:** sapphire test masses and fused silica auxiliary optics.
- Different materials have different responses to the vector field (different q/M of the mirrors)
- The differential strain is enhanced

$$\sqrt{\langle h_D^2 \rangle} = C \frac{q}{M} \frac{e\epsilon}{2\pi c^2} \sqrt{\frac{2\rho_{\text{DM}}}{\epsilon_0} \frac{v_0}{f_0}}$$

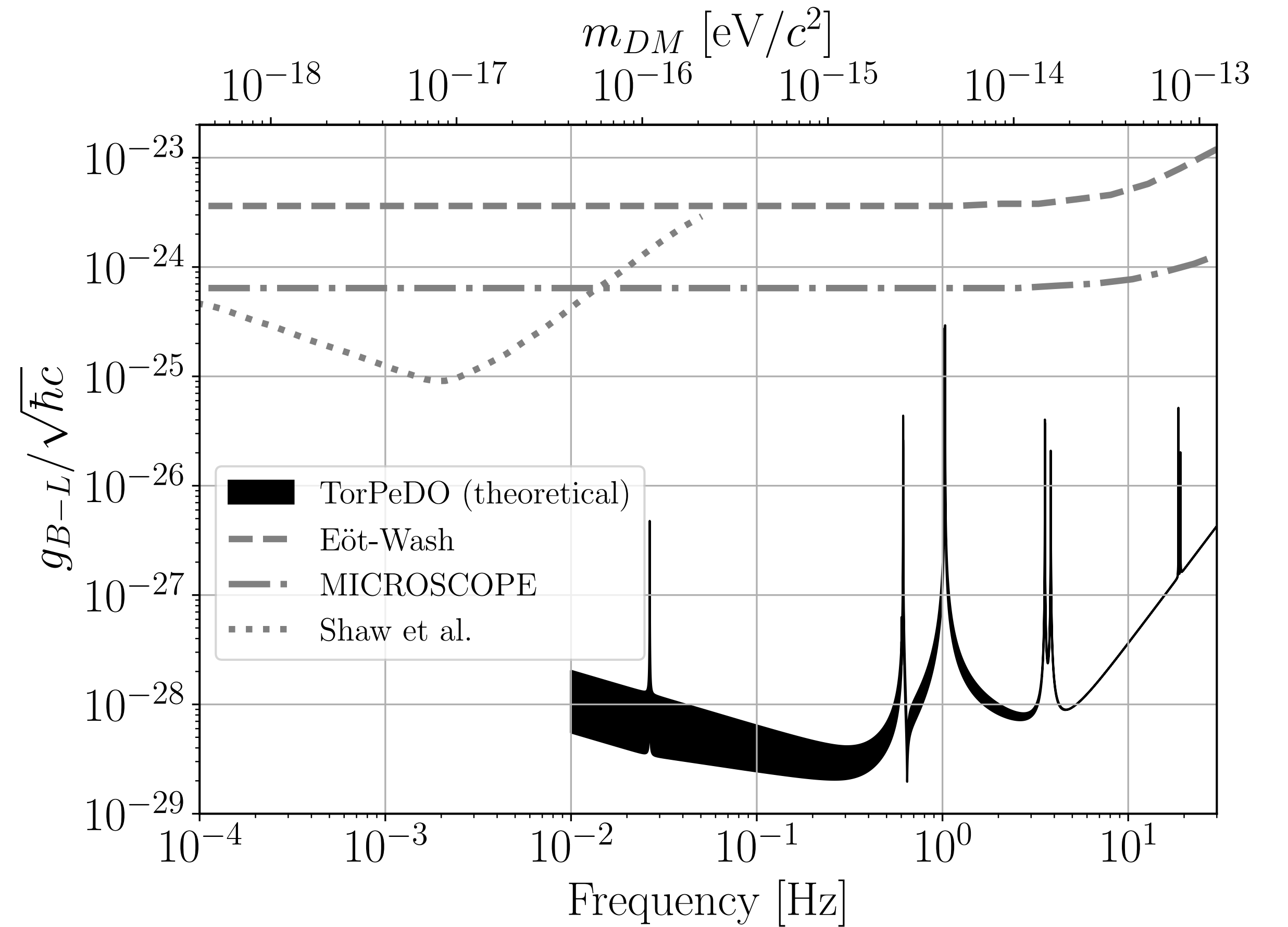
Michimura et al., PRD102, 102001 (2020);
 Nakatsuka et al. PRD108, 092010 (2022);
 LVK, [arXiv:2403.03004](https://arxiv.org/abs/2403.03004)



TorPeDo



$$\sqrt{\langle \delta \tau_A^2 \rangle} \simeq \frac{M}{m_n} \Delta_{B-L} g_{B-L} r \sqrt{\rho_{DM}},$$



Sun et al. [arXiv:2402.08935](https://arxiv.org/abs/2402.08935)

Boson Clouds

Boson clouds

See the extensive literature:

Arvanitaki et al., PRD 81, 123530 (2010); PRD 83, 044026 (2011); PRD 91, 084011 (2015)

Brito et al., Lect. Not. Phys. 971 (2020); PRL 124, 211101 (2020)

Baryakhtar et al. PRD 96, 035019 (2017); PRD 103, 095019 (2021)

Siemonsen & East, 101, 024019 (2020)

...

Boson clouds

See the extensive literature:

Arvanitaki et al., PRD 81, 123530 (2010); PRD 83, 044026 (2011); PRD 91, 084011 (2015)

Brito et al., Lect. Not. Phys. 971 (2020); PRL 124, 211101 (2020)

Baryakhtar et al. PRD 96, 035019 (2017); PRD 103, 095019 (2021)

Siemonsen & East, 101, 024019 (2020)

...

- Ultralight bosonic particles (scalar, vector or tensor fields; QCD axion, axion-like particles) can clump around spinning BHs due to **superradiance**

Boson clouds

See the extensive literature:

Arvanitaki et al., PRD 81, 123530 (2010); PRD 83, 044026 (2011); PRD 91, 084011 (2015)

Brito et al., Lect. Not. Phys. 971 (2020); PRL 124, 211101 (2020)

Baryakhtar et al. PRD 96, 035019 (2017); PRD 103, 095019 (2021)

Siemonsen & East, 101, 024019 (2020)

...

- Ultralight bosonic particles (scalar, vector or tensor fields; QCD axion, axion-like particles) can clump around spinning BHs due to **superradiance**
- Given a BH with (M_{BH}, χ_i) and a boson particle of m_b , the superradiance instability is maximized if the **confinement conditions** are satisfied $\hbar c/m_b \sim 2GM_{\text{BH}}/c^2$

Boson clouds

See the extensive literature:

Arvanitaki et al., PRD 81, 123530 (2010); PRD 83, 044026 (2011); PRD 91, 084011 (2015)

Brito et al., Lect. Not. Phys. 971 (2020); PRL 124, 211101 (2020)

Baryakhtar et al. PRD 96, 035019 (2017); PRD 103, 095019 (2021)

Siemonsen & East, 101, 024019 (2020)

...

- Ultralight bosonic particles (scalar, vector or tensor fields; QCD axion, axion-like particles) can clump around spinning BHs due to **superradiance**
- Given a BH with (M_{BH}, χ_i) and a boson particle of m_b , the superradiance instability is maximized if the **confinement conditions** are satisfied $\hbar c/m_b \sim 2GM_{\text{BH}}/c^2$
- Astrophysical BHs could match well with boson masses ranging from 10^{-20} to 10^{-10} eV

Boson clouds

See the extensive literature:

Arvanitaki et al., PRD 81, 123530 (2010); PRD 83, 044026 (2011); PRD 91, 084011 (2015)

Brito et al., Lect. Not. Phys. 971 (2020); PRL 124, 211101 (2020)

Baryakhtar et al. PRD 96, 035019 (2017); PRD 103, 095019 (2021)

Siemonsen & East, 101, 024019 (2020)

...

- Ultralight bosonic particles (scalar, vector or tensor fields; QCD axion, axion-like particles) can clump around spinning BHs due to **superradiance**
- Given a BH with (M_{BH}, χ_i) and a boson particle of m_b , the superradiance instability is maximized if the **confinement conditions** are satisfied $\hbar c/m_b \sim 2GM_{\text{BH}}/c^2$
- Astrophysical BHs could match well with boson masses ranging from 10^{-20} to 10^{-10} eV
- Potentially observable through their effects on the BH's **dynamics** and the **gravitational waves** they emit

Boson clouds

See the extensive literature:

Arvanitaki et al., PRD 81, 123530 (2010); PRD 83, 044026 (2011); PRD 91, 084011 (2015)

Brito et al., Lect. Not. Phys. 971 (2020); PRL 124, 211101 (2020)

Baryakhtar et al. PRD 96, 035019 (2017); PRD 103, 095019 (2021)

Siemonsen & East, 101, 024019 (2020)

...

- Ultralight bosonic particles (scalar, vector or tensor fields; QCD axion, axion-like particles) can clump around spinning BHs due to **superradiance**
- Given a BH with (M_{BH}, χ_i) and a boson particle of m_b , the superradiance instability is maximized if the **confinement conditions** are satisfied $\hbar c/m_b \sim 2GM_{\text{BH}}/c^2$
- Astrophysical BHs could match well with boson masses ranging from 10^{-20} to 10^{-10} eV
- Potentially observable through their effects on the BH's **dynamics** and the **gravitational waves** they emit
- The gravitational wave **frequency f_{GW}** is mainly determined by the **boson mass**

Boson clouds

See the extensive literature:

Arvanitaki et al., PRD 81, 123530 (2010); PRD 83, 044026 (2011); PRD 91, 084011 (2015)

Brito et al., Lect. Not. Phys. 971 (2020); PRL 124, 211101 (2020)

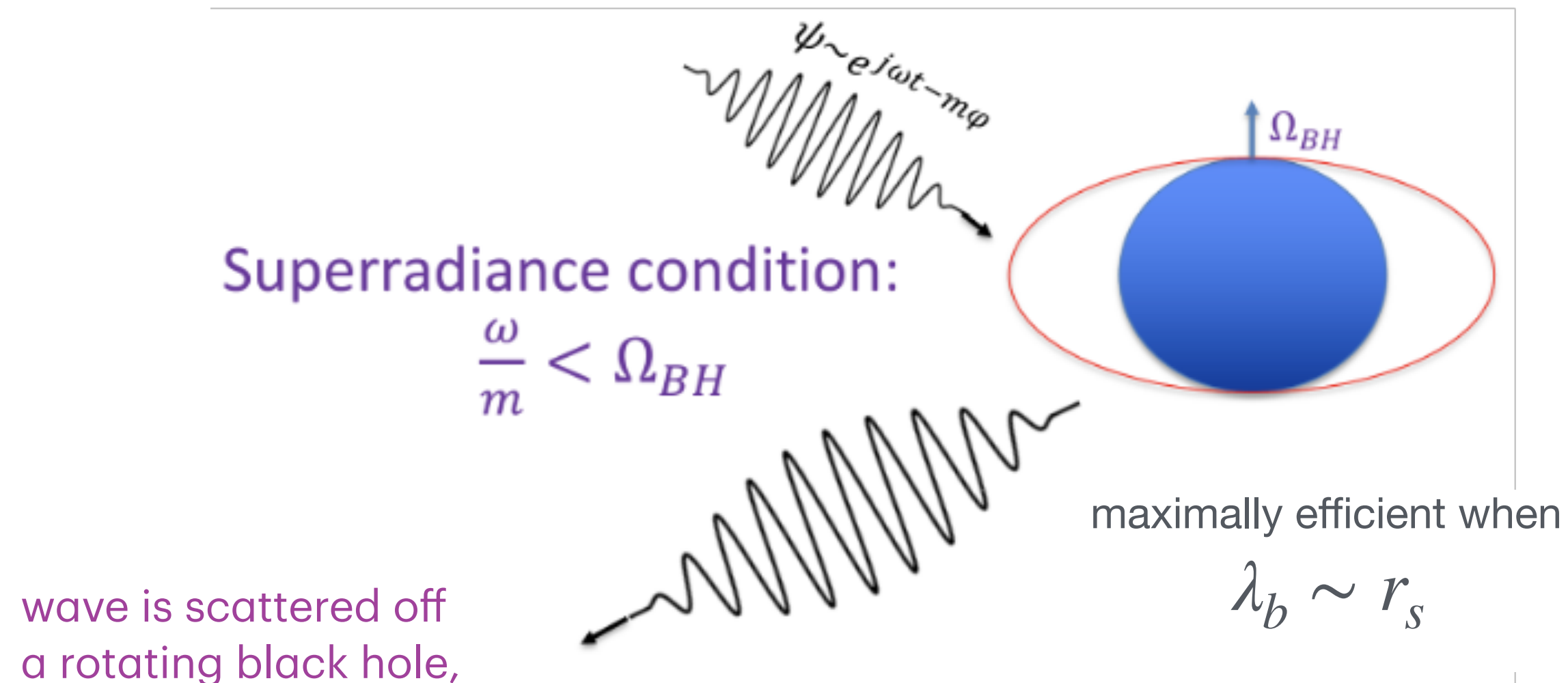
Baryakhtar et al. PRD 96, 035019 (2017); PRD 103, 095019 (2021)

Siemonsen & East, 101, 024019 (2020)

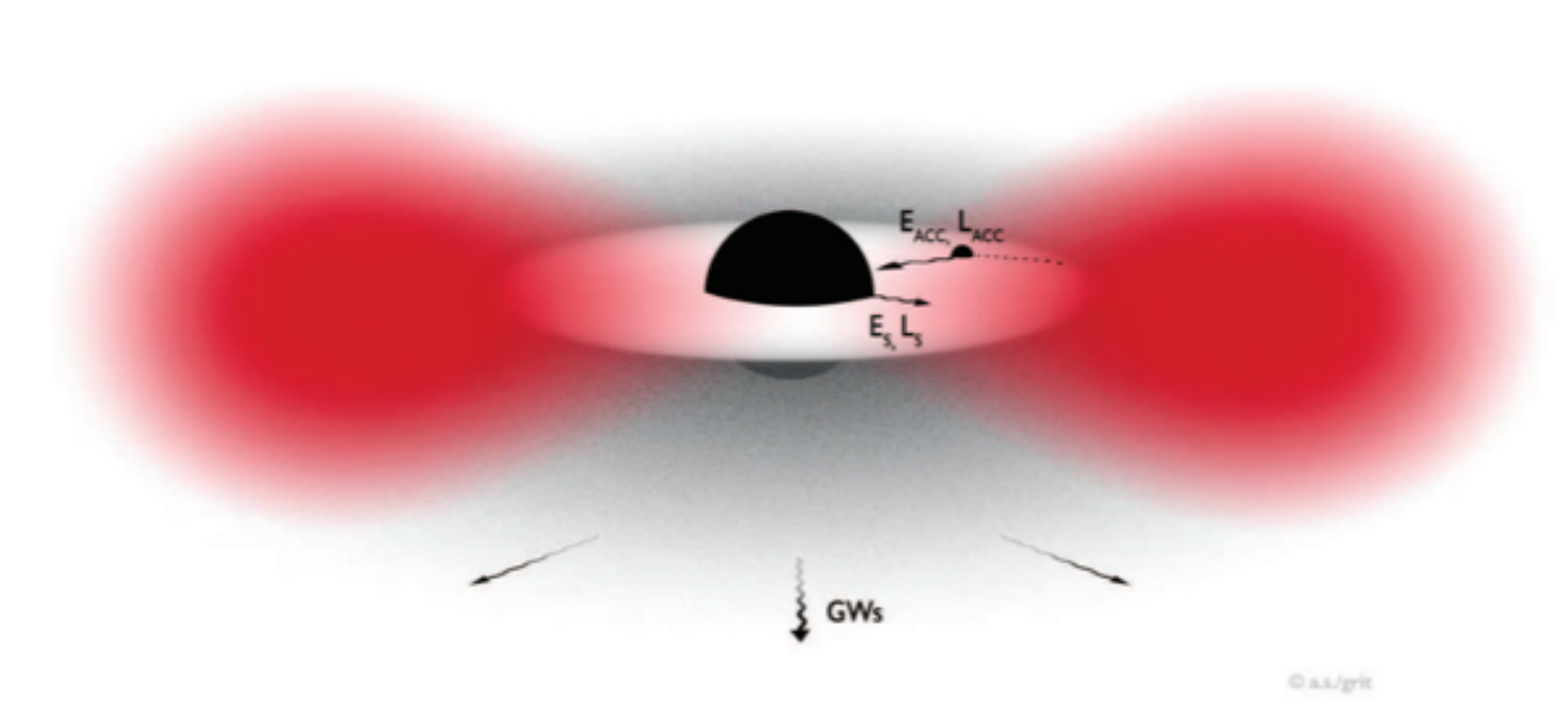
...

- Ultralight bosonic particles (scalar, vector or tensor fields; QCD axion, axion-like particles) can clump around spinning BHs due to **superradiance**
- Given a BH with (M_{BH}, χ_i) and a boson particle of m_b , the superradiance instability is maximized if the **confinement conditions** are satisfied $\hbar c/m_b \sim 2GM_{\text{BH}}/c^2$
- Astrophysical BHs could match well with boson masses ranging from 10^{-20} to 10^{-10} eV
- Potentially observable through their effects on the BH's **dynamics** and the **gravitational waves** they emit
- The gravitational wave **frequency f_{GW}** is mainly determined by the **boson mass**
- LIGO/Virgo/KAGRA are sensitive to a mass range of **10^{-14} to 10^{-11} eV** (10-2000 Hz)

Boson clouds



wave is scattered off a rotating black hole, energy and angular momentum are extracted from a BH leading to the amplification of these fields.



- We need: boson angular frequency < BH's outer horizon angular frequency for the growth
- field bosons condensate, occupying the same (quantum) state with huge occupation numbers
- This process (~mins-days) subtracts energy from the BH momentum -> The BH slows down
- The superradiance stops (at saturation) and the cloud dissipates through GWs (~days-years)

[Picture credit: Ana Sousa Carvalho]

The boson cloud signal

- The BH-boson cloud system resembles the hydrogen atom = *gravitational atom*



fine structure constant

$$\alpha = \frac{GM_{\text{BH}}}{c^3} \frac{m_b}{\hbar}$$

- The strain amplitude decays as $h(t) = \frac{h_0}{1 + \frac{t}{\tau_{\text{gw}}}}$

- The GW frequency is twice the field frequency

$$f_{\text{GW}} \approx 645 \text{ Hz} \left(\frac{10 M_{\odot}}{M_{\text{BH}}} \right) \left(\frac{\alpha}{0.1} \right) \quad (\text{at 1st order})$$

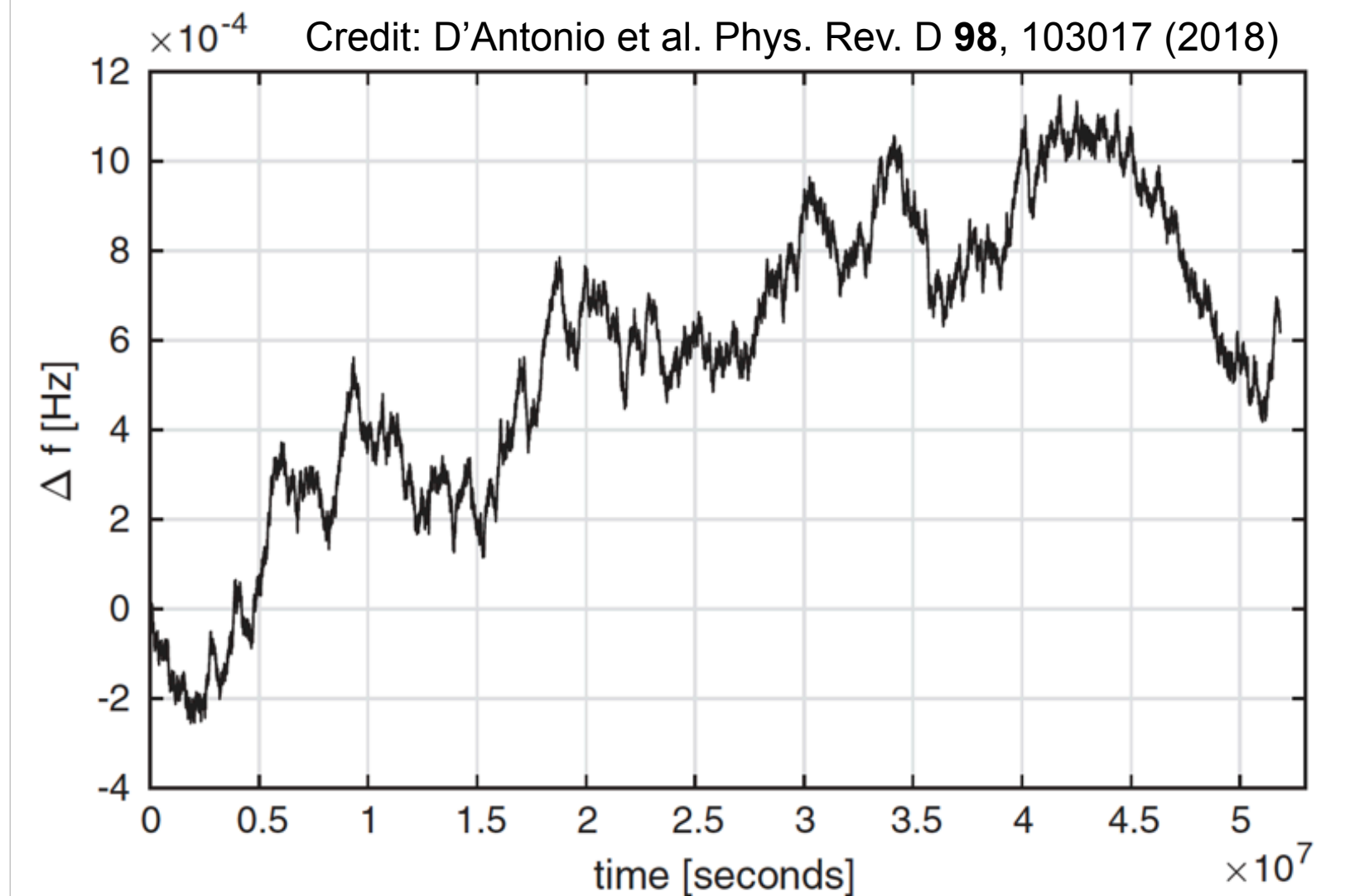
- A small spin-up due to annihilation is present

scalar

vector

$$\dot{f} \approx 3 \times 10^{-14} \text{ Hz/s} \left(\frac{10 M_{\odot}}{M_{\text{BH}}} \right)^2 \left(\frac{\alpha}{0.1} \right)^{19} \chi_i^2 \quad \left| \quad \dot{f} \approx 1 \times 10^{-6} \text{ Hz/s} \left(\frac{10 M_{\odot}}{M_{\text{BH}}} \right)^2 \left(\frac{\alpha}{0.1} \right)^{15} \chi_i^2$$

We do not consider the effect due to transition levels



(when self interaction is negligible)

see Collaviti et al. [arXiv:2407.04304](https://arxiv.org/abs/2407.04304)

Scalar boson clouds methods and searches (CW-like)

Scalar boson clouds methods and searches (CW-like)

- First **all-sky survey**. Frequency **20–610 Hz** (O3 LIGO data). Small **spin-up** range around zero - Abbott et al. PRD 105, 102001 (2022) (see also Palomba et al. PRL 123 171101 (2019) - O2 data; Dergachev and Papa PRL 123 101101 (2019) - O1 data). All-sky semi-coherent method: D'Antonio PRD 98, 103017 (2018);

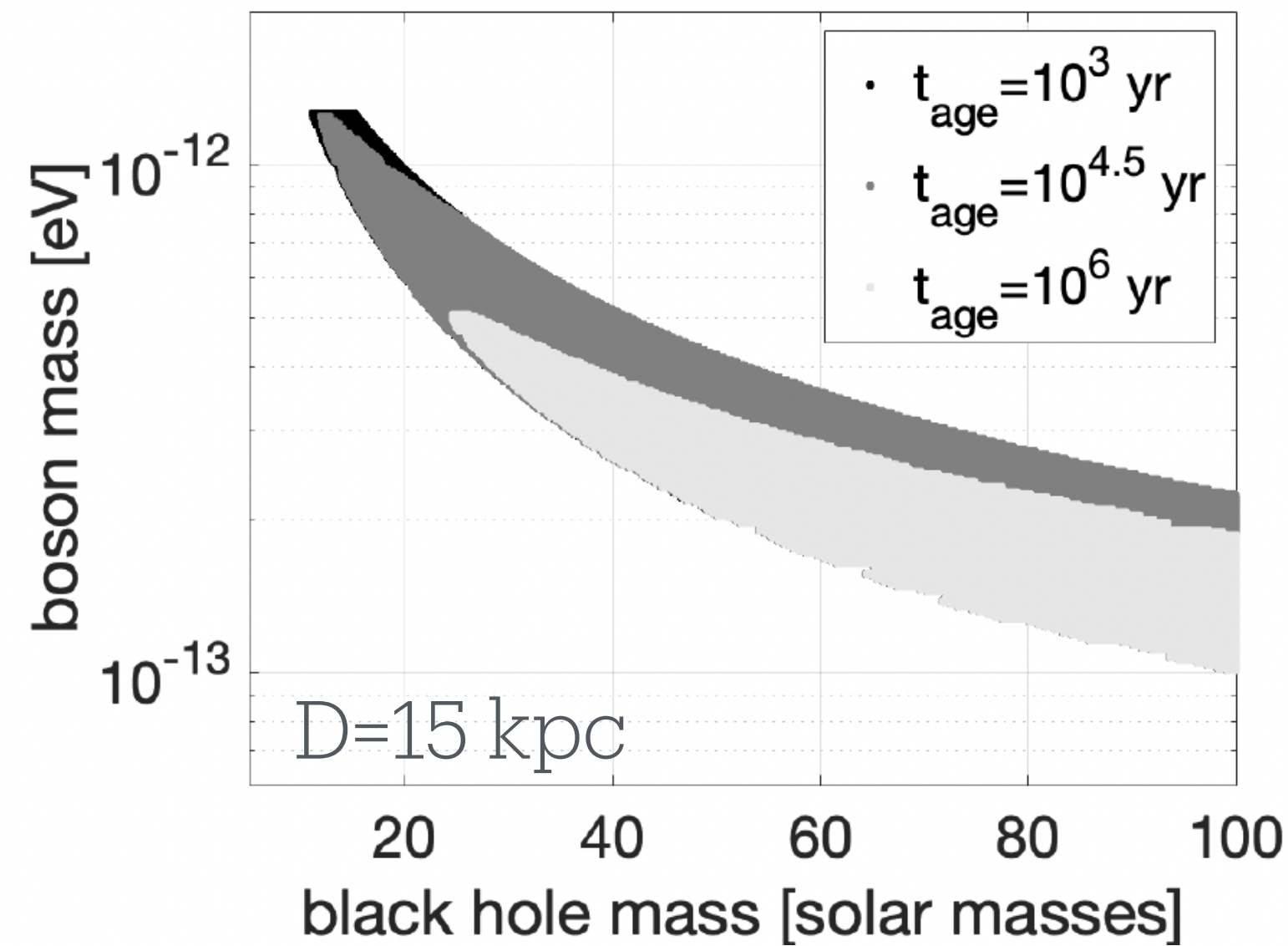
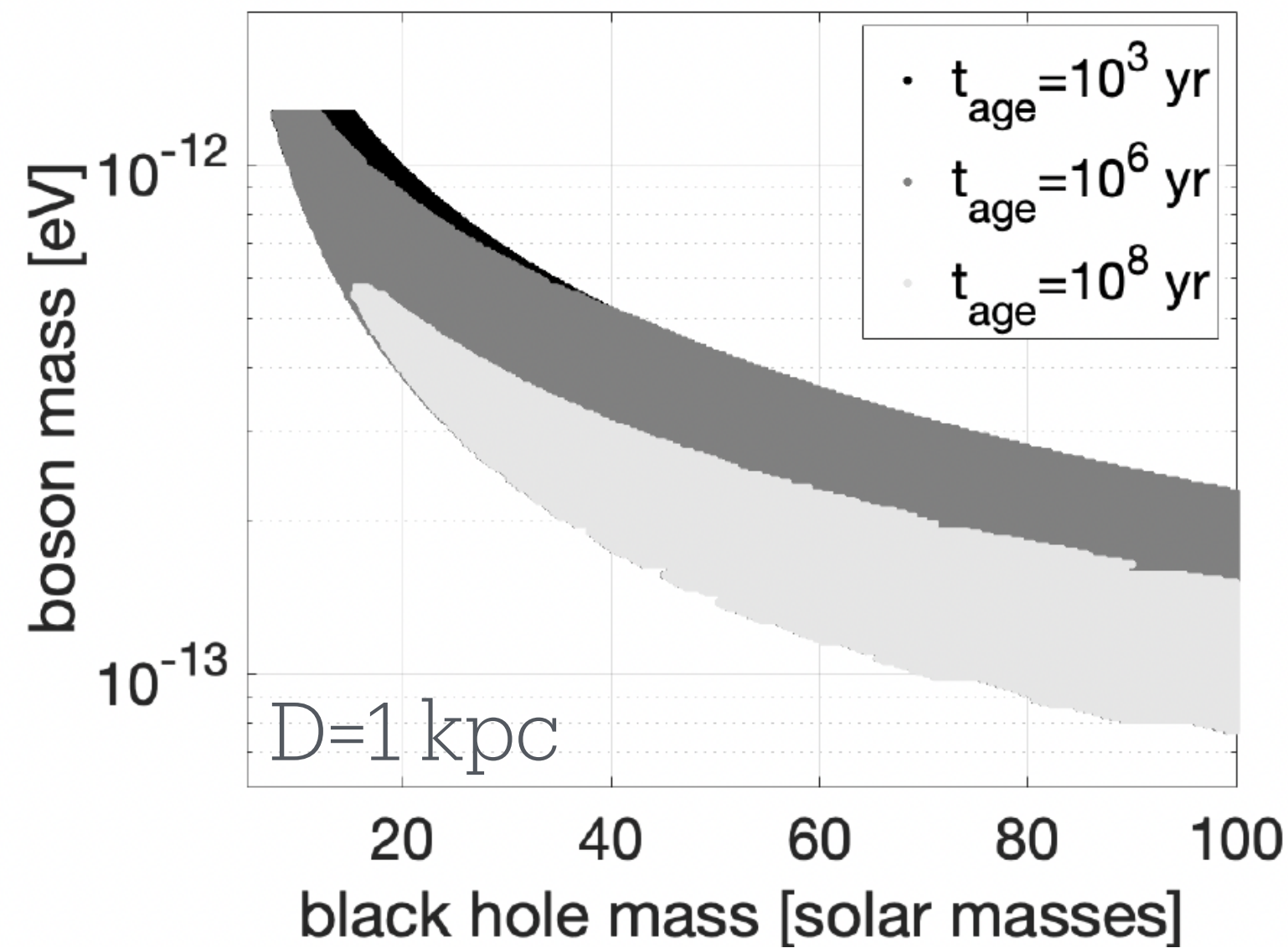
Scalar boson clouds methods and searches (CW-like)

- First **all-sky survey**. Frequency **20–610 Hz** (O3 LIGO data). Small **spin-up** range around zero - Abbott et al. PRD 105, 102001 (2022) (see also Palomba et al. PRL 123 171101 (2019) - O2 data; Dergachev and Papa PRL 123 101101 (2019) - O1 data). All-sky semi-coherent method: D'Antonio PRD 98, 103017 (2018);
- **Ensemble of signals**, characterization and impact on CW analyses: Zhu, et al., PRD 102, 063020 (2020); Pierini, et al., PRD 106, 042009 (2022)

Scalar boson clouds methods and searches (CW-like)

- First **all-sky survey**. Frequency **20–610 Hz** (O3 LIGO data). Small **spin-up** range around zero - Abbott et al. PRD 105, 102001 (2022) (see also Palomba et al. PRL 123 171101 (2019) - O2 data; Dergachev and Papa PRL 123 101101 (2019) - O1 data). All-sky semi-coherent method: D'Antonio PRD 98, 103017 (2018);
- **Ensemble of signals**, characterization and impact on CW analyses: Zhu, et al., PRD 102, 063020 (2020); Pierini, et al., PRD 106, 042009 (2022)
- Directed:
 - ✦ targeting the **Galactic Center** in O3 data: no priors on BH mass, spin or ages - Abbott et al. PRD 106, 042003 (2022); semi-coherent method in Piccinni et al., PRD 101, 082004 (2020)
 - ✦ targeting known **galactic BHs: Cygnus X-1** O2 - rely on the mass, spin and age estimates of the target - Sun et al. PRD 101, 063020 (2020); Hidden Markov model tracking (directed) Isi et al. PRD 99 084042 (2019);

Exclusion regions LVK, PRD 105, 102001 (2022)



BH spin = 0.9

$$h_0 \approx 6 \times 10^{-24} \left(\frac{M_{\text{BH}}}{10 M_{\odot}} \right) \left(\frac{\alpha}{0.1} \right)^7 \left(\frac{1 \text{ kpc}}{D} \right) (\chi_i - \chi_c)$$

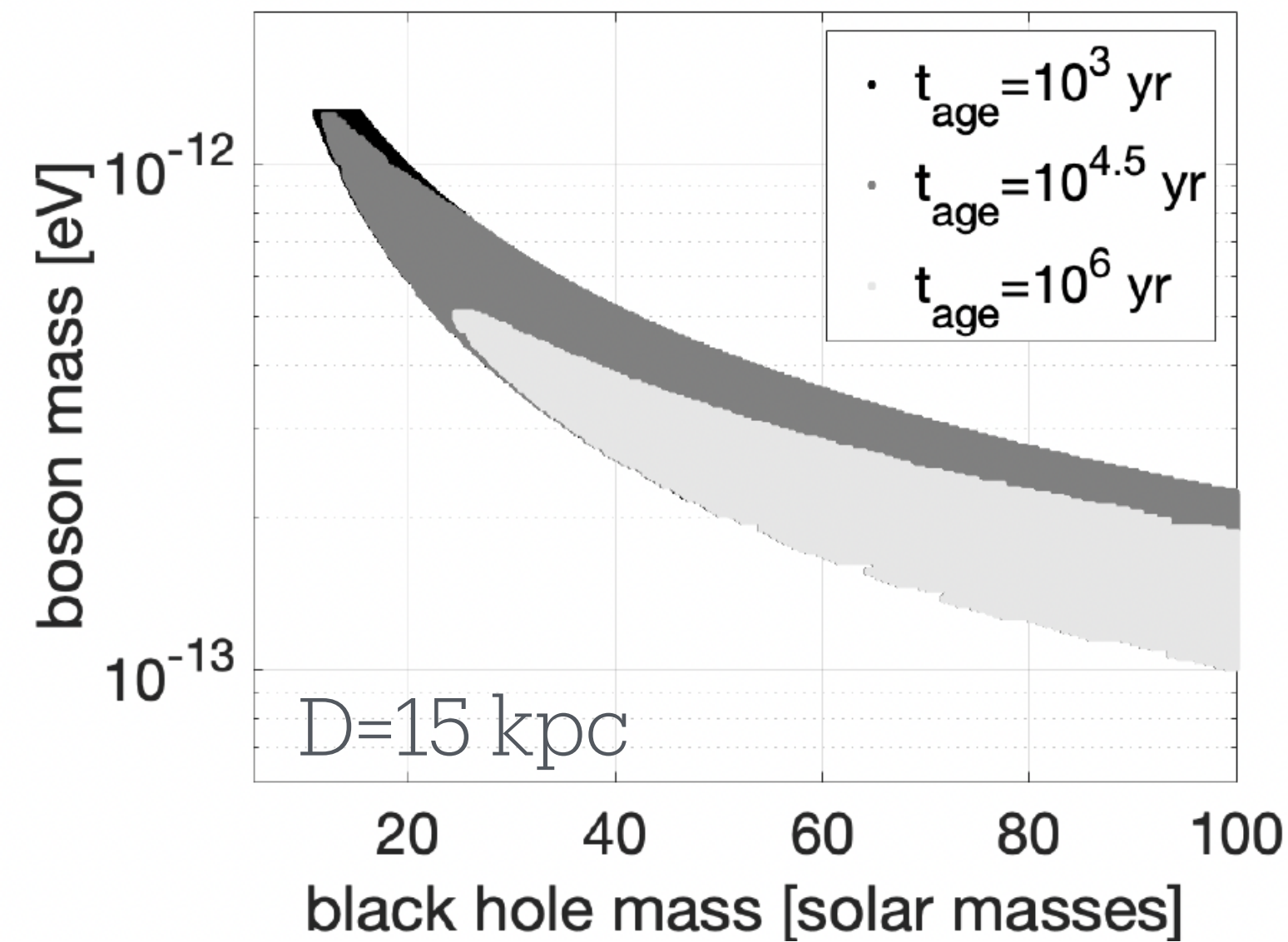
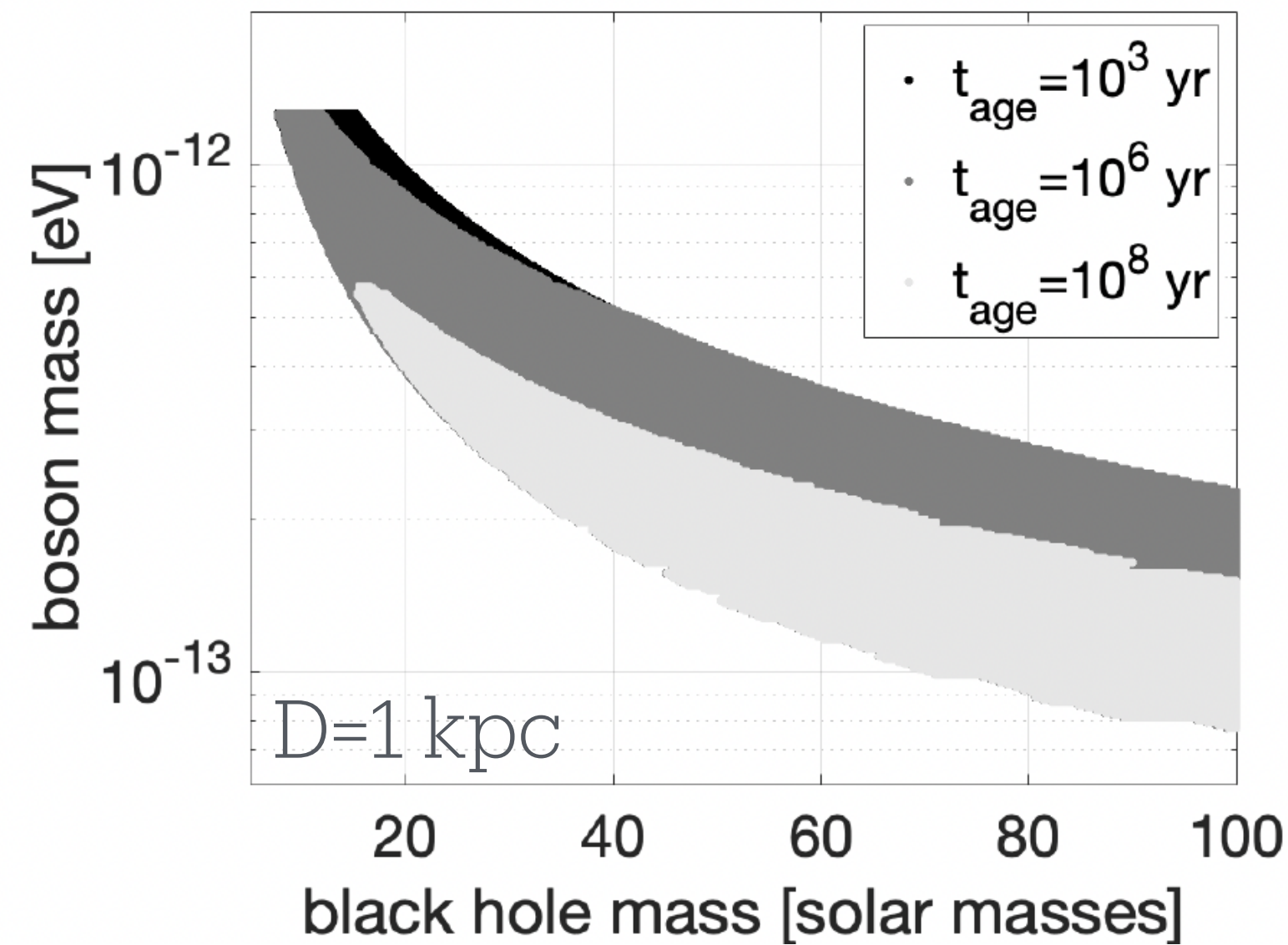
$$h(t) = \frac{h_0}{1 + \frac{t}{\tau_{\text{gw}}}}$$

assuming a BH with a given spin, distance and age



we exclude some BH-boson masses combination

Exclusion regions LVK, PRD 105, 102001 (2022)



BH spin = 0.9

$$h_0 \approx 6 \times 10^{-24} \left(\frac{M_{\text{BH}}}{10 M_{\odot}} \right) \left(\frac{\alpha}{0.1} \right)^7 \left(\frac{1 \text{ kpc}}{D} \right) (\chi_i - \chi_c)$$

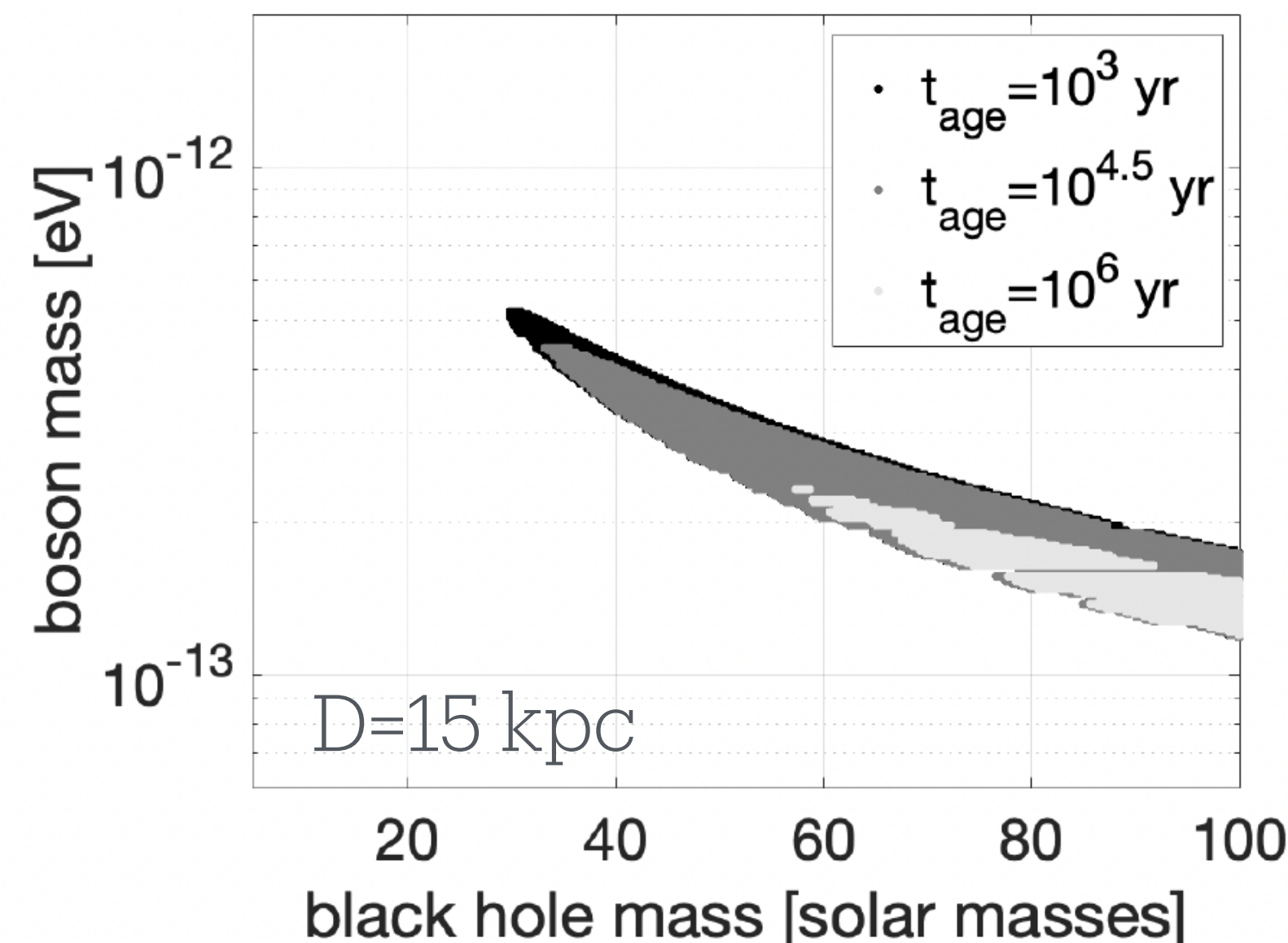
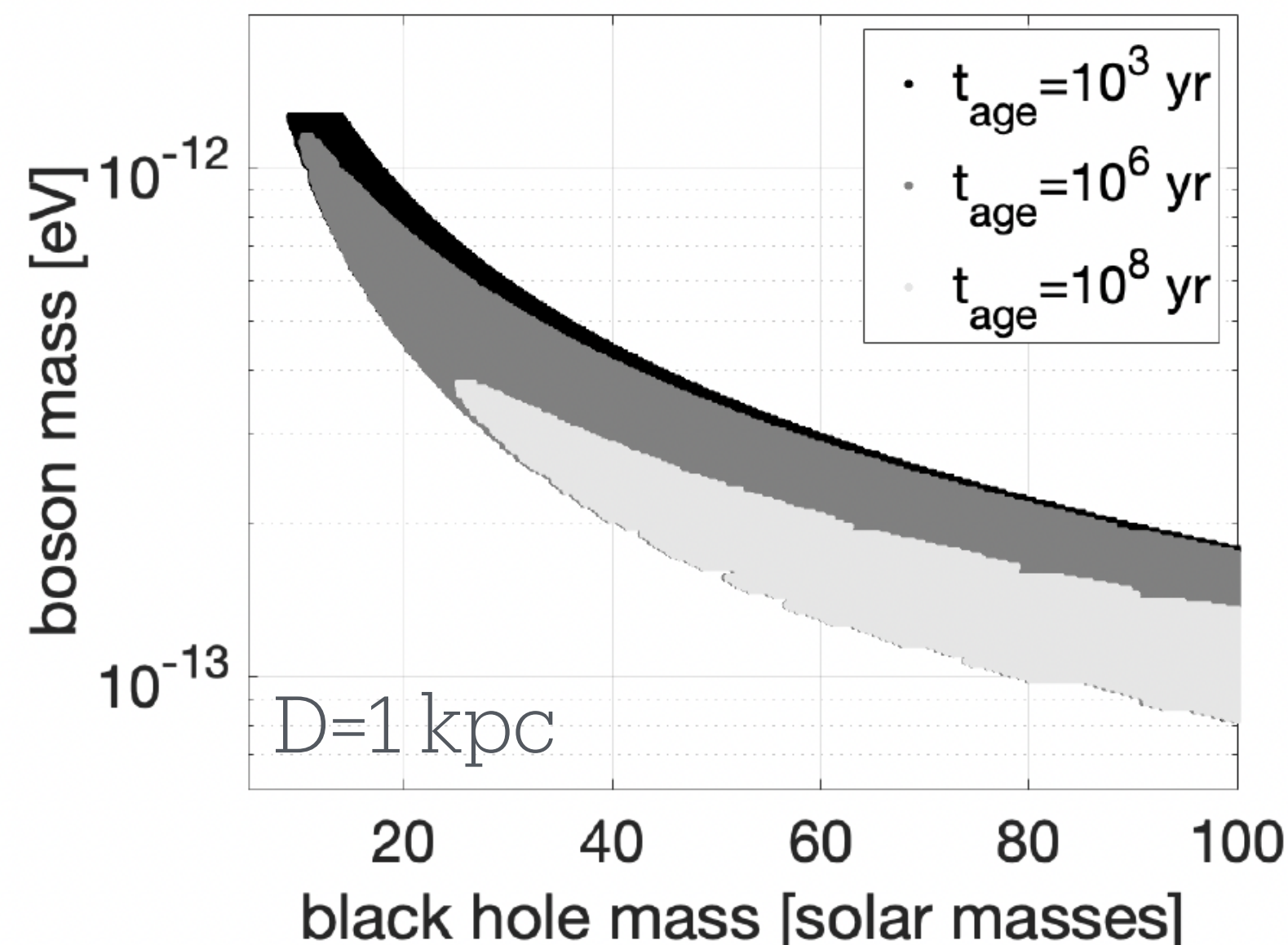
$$h(t) = \frac{h_0}{1 + \frac{t}{\tau_{\text{gw}}}}$$

assuming a BH with a given spin, distance and age



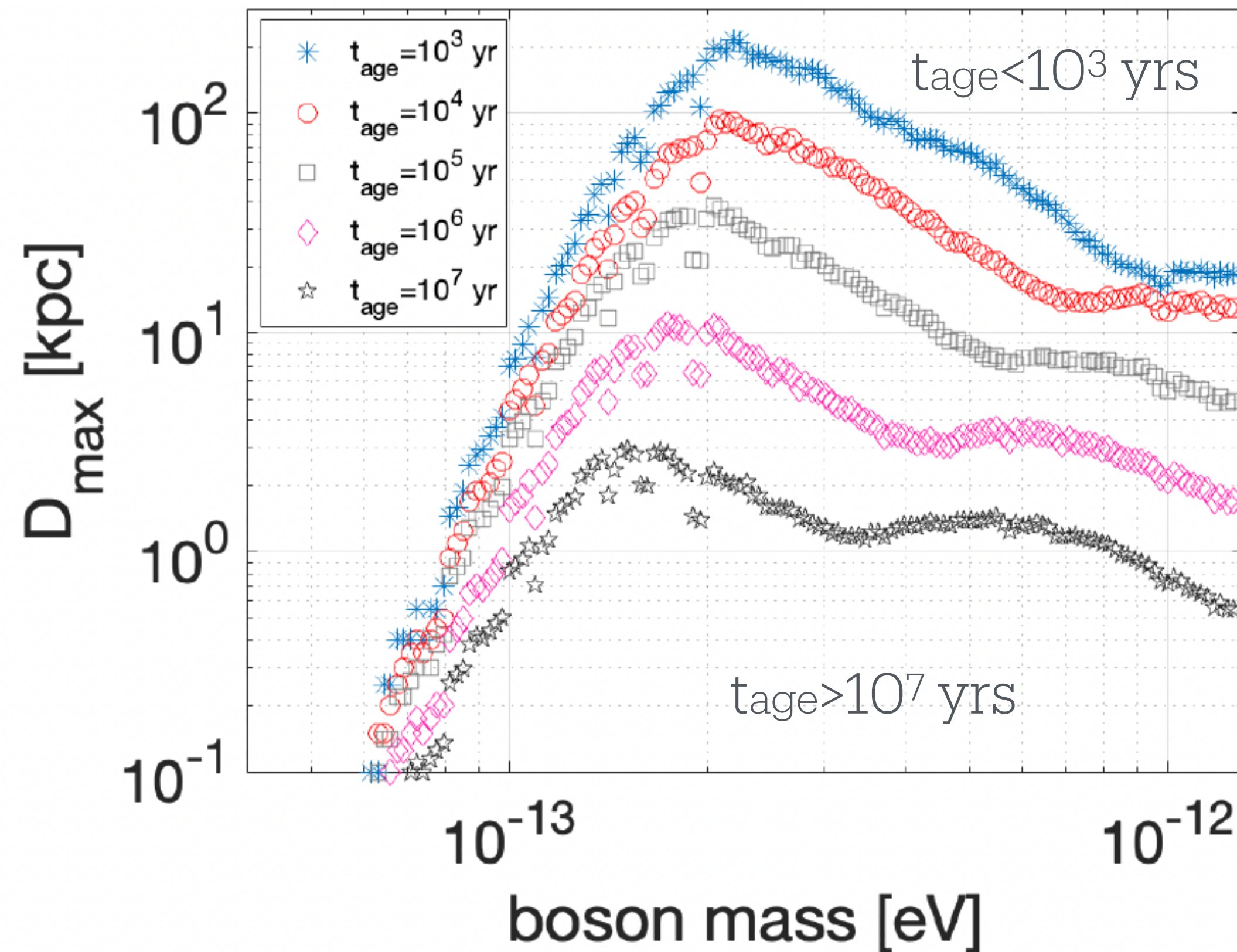
we exclude some BH-boson masses combination

BH spin = 0.5



Astrophysical reach of the search LVK, PRD 105, 102001 (2022)

maximum distance at which a given BH–boson cloud system, with a certain age, is not emitting CWs, as a function of the boson mass



Simulating a BH population with:

- Kroupa mass distribution $[5, 100] M_{\odot}$
- uniform spin distribution $[0.2, 0.9]$.

A similar trend for a simulated BH population of $[5, 50] M_{\odot}$.

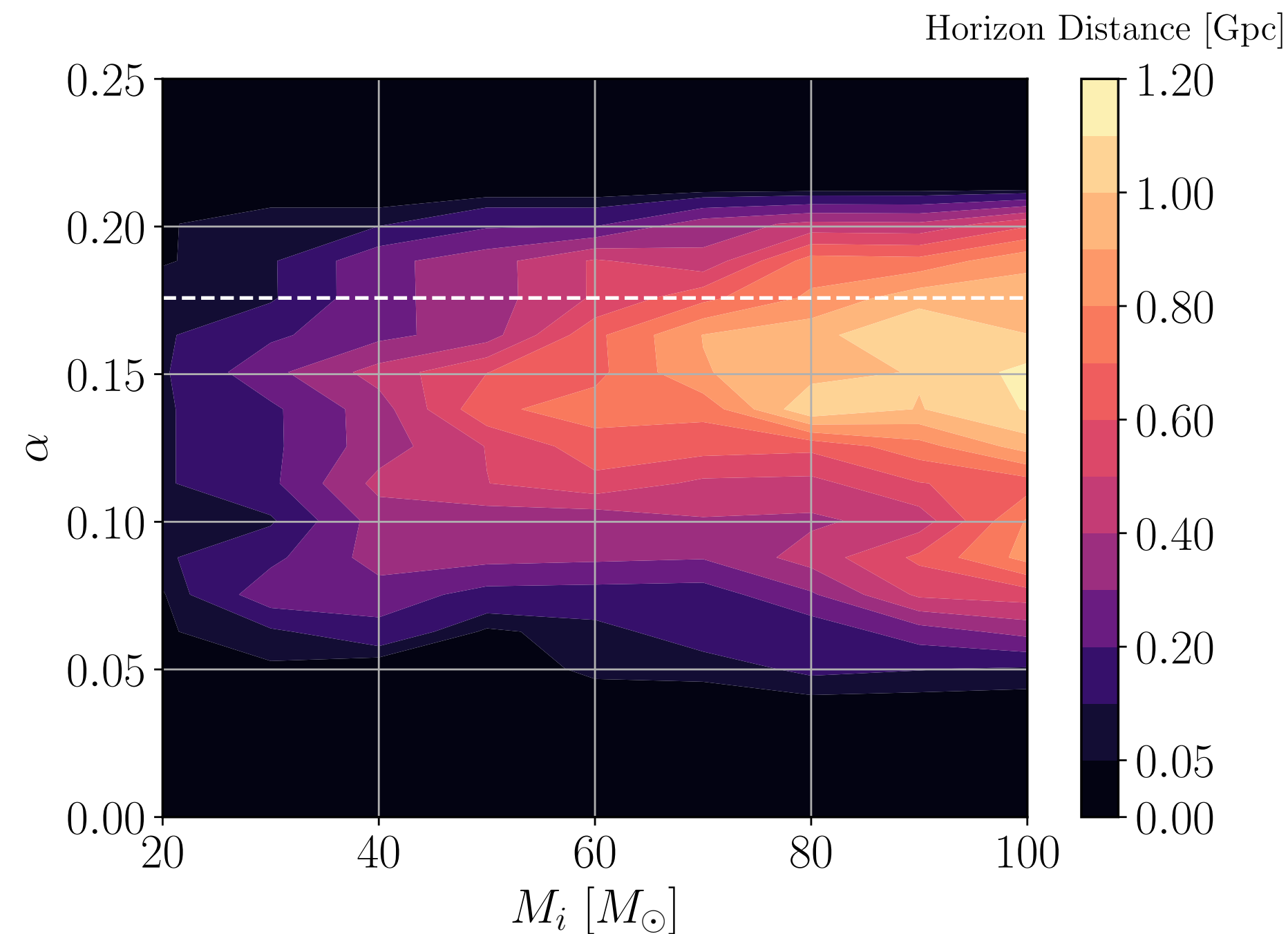
Results depend on the properties of the simulated BH population.

Vector boson clouds in post-merger remnant BHs

Horizon distances

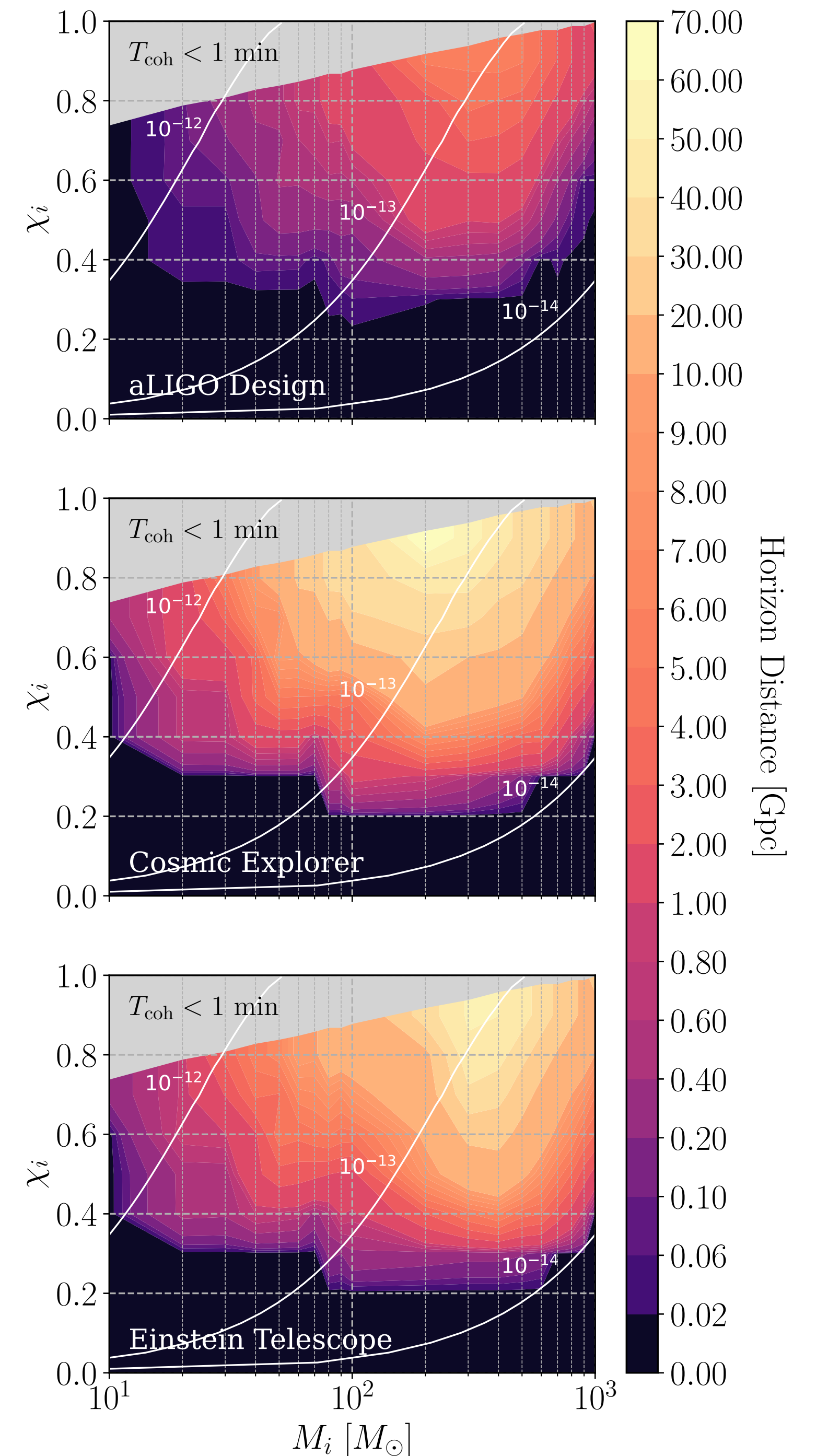
Hidden Markov model tracking signals on timescales from hours to months.

Jones et al., PRD 108, 064001 (2023)



Able to reach signals at a luminosity distance above ~1 Gpc (in current gen.)

Scalar clouds in CBC remnant are not promising in current gen. detectors



Other ways to look for BC evidence

(other than CW methods)

Other ways to look for BC evidence

(other than CW methods)

- Impact of DM on **binary dynamics** - Baumann et al., PRD99, 044001 (2019); Hannuksela et al. Nature Astron. 3 447 (2019); Xue, Huang, Sci. China Phys., Mech. & Astro., 67 210411 (2024)

Other ways to look for BC evidence

(other than CW methods)

- Impact of DM on **binary dynamics** - Baumann et al., PRD99, 044001 (2019); Hannuksela et al. Nature Astron. 3 447 (2019); Xue, Huang, Sci. China Phys., Mech. & Astro., 67 210411 (2024)
- **Stochastic background** generated by the superposition of all signals from **scalar or vector** boson cloud; Assume BH spin distribution and merger rate - Tsukada et al., PRD 103, 082005 (2021): Vector boson clouds (O1+O2); Yuan et al., PRD106, 023020 (2022): Scalar boson clouds (O1+O2+O3)

Other ways to look for BC evidence

(other than CW methods)

- Impact of DM on **binary dynamics** - Baumann et al., PRD99, 044001 (2019); Hannuksela et al. Nature Astron. 3 447 (2019); Xue, Huang, Sci. China Phys., Mech. & Astro., 67 210411 (2024)
- **Stochastic background** generated by the superposition of all signals from **scalar or vector** boson cloud; Assume BH spin distribution and merger rate - Tsukada et al., PRD 103, 082005 (2021): Vector boson clouds (O1+O2); Yuan et al., PRD106, 023020 (2022): Scalar boson clouds (O1+O2+O3)
- SGWB from **tensor** boson clouds - Guo et al. Arxiv 2312.16435

Other ways to look for BC evidence

(other than CW methods)

- Impact of DM on **binary dynamics** - Baumann et al., PRD99, 044001 (2019); Hannuksela et al. Nature Astron. 3 447 (2019); Xue, Huang, Sci. China Phys., Mech. & Astro., 67 210411 (2024)
- **Stochastic background** generated by the superposition of all signals from **scalar or vector** boson cloud; Assume BH spin distribution and merger rate - Tsukada et al., PRD 103, 082005 (2021): Vector boson clouds (O1+O2); Yuan et al., PRD106, 023020 (2022): Scalar boson clouds (O1+O2+O3)
- SGWB from **tensor** boson clouds - Guo et al. Arxiv 2312.16435
- Constraints from **BH spin distributions** (spin limited by superradiance) - Ng et al., PRL 126, 151102 (2021)

Other ways to look for BC evidence

(other than CW methods)

- Impact of DM on **binary dynamics** - Baumann et al., PRD99, 044001 (2019); Hannuksela et al. Nature Astron. 3 447 (2019); Xue, Huang, Sci. China Phys., Mech. & Astro., 67 210411 (2024)
- **Stochastic background** generated by the superposition of all signals from **scalar or vector** boson cloud; Assume BH spin distribution and merger rate - Tsukada et al., PRD 103, 082005 (2021): Vector boson clouds (O1+O2); Yuan et al., PRD106, 023020 (2022): Scalar boson clouds (O1+O2+O3)
- SGWB from **tensor** boson clouds - Guo et al. Arxiv 2312.16435
- Constraints from **BH spin distributions** (spin limited by superradiance) - Ng et al., PRL 126, 151102 (2021)
- Effects on the GW waveform due to **boson transfer** BBH system - Guo et al. 2309.07790

Other ways to look for BC evidence

(other than CW methods)

- Impact of DM on **binary dynamics** - Baumann et al., PRD99, 044001 (2019); Hannuksela et al. Nature Astron. 3 447 (2019); Xue, Huang, Sci. China Phys., Mech. & Astro., 67 210411 (2024)
- **Stochastic background** generated by the superposition of all signals from **scalar or vector** boson cloud; Assume BH spin distribution and merger rate - Tsukada et al., PRD 103, 082005 (2021): Vector boson clouds (O1+O2); Yuan et al., PRD106, 023020 (2022): Scalar boson clouds (O1+O2+O3)
- SGWB from **tensor** boson clouds - Guo et al. Arxiv 2312.16435
- Constraints from **BH spin distributions** (spin limited by superradiance) - Ng et al., PRL 126, 151102 (2021)
- Effects on the GW waveform due to **boson transfer** BBH system - Guo et al. 2309.07790
- Checking the rates of **hierarchical black hole mergers** in nuclear star clusters - Payne et al 2022 ApJ 931 79 (2022)

Conclusion

- Earth-based interferometers can be used to look for DM evidence as a GW signal or as direct detectors
- Searches in GW data are already providing **interesting constraints** in the ultralight mass range
- New DA techniques are under development, improving also in the **signal modeling**
- There is a wide margin of improvement if we consider second-order effects, different self-interaction regimes, etc...
- In the case of detection, it might be difficult to **distinguish between sources** (e.g. NS or BC?) and **between signal models** (scalar, vector, tensor, self-interaction or not, relativistic regime, ...)
- We look forward to the upcoming O4 run!

Backup

Scalar vs Vector: timescales and h_0

Scalar bosons

$$\tau_{\text{inst}} \approx 20 \text{ days} \left(\frac{M_{\text{BH}}}{10 M_{\odot}} \right) \left(\frac{0.1}{\alpha} \right)^9 \frac{1}{\chi_i}$$

$$\tau_{\text{GW}} \approx 10^5 \text{ yr} \left(\frac{M_{\text{BH}}}{10 M_{\odot}} \right) \left(\frac{0.1}{\alpha} \right)^{15} \left(\frac{0.5}{\chi_i - \chi_f} \right)$$

$$h_0 \approx 6 \times 10^{-24} \left(\frac{M_{\text{BH}}}{10 M_{\odot}} \right) \left(\frac{\alpha}{0.1} \right)^7 \left(\frac{1 \text{ kpc}}{d} \right) (\chi_i - \chi_f)$$

Vector bosons

$$\tau_{\text{inst}} \approx 2 \text{ mins} \left(\frac{M_{\text{BH}}}{10 M_{\odot}} \right) \left(\frac{0.1}{\alpha} \right)^7 \frac{1}{\chi_i}$$

$$\tau_{\text{GW}} \approx 8 \text{ days} \left(\frac{M_{\text{BH}}}{10 M_{\odot}} \right) \left(\frac{0.1}{\alpha} \right)^{11} \left(\frac{0.5}{\chi_i - \chi_f} \right)$$

$$h_0 \approx 3 \times 10^{-26} \left(\frac{M}{10 M_{\odot}} \right) \left(\frac{\alpha}{0.1} \right)^5 \left(\frac{1 \text{ Gpc}}{d} \right) (\chi_i - \chi_f)$$

Valid in the non relativistic regime

Scalar vs Vector: Frequency

Scalar bosons

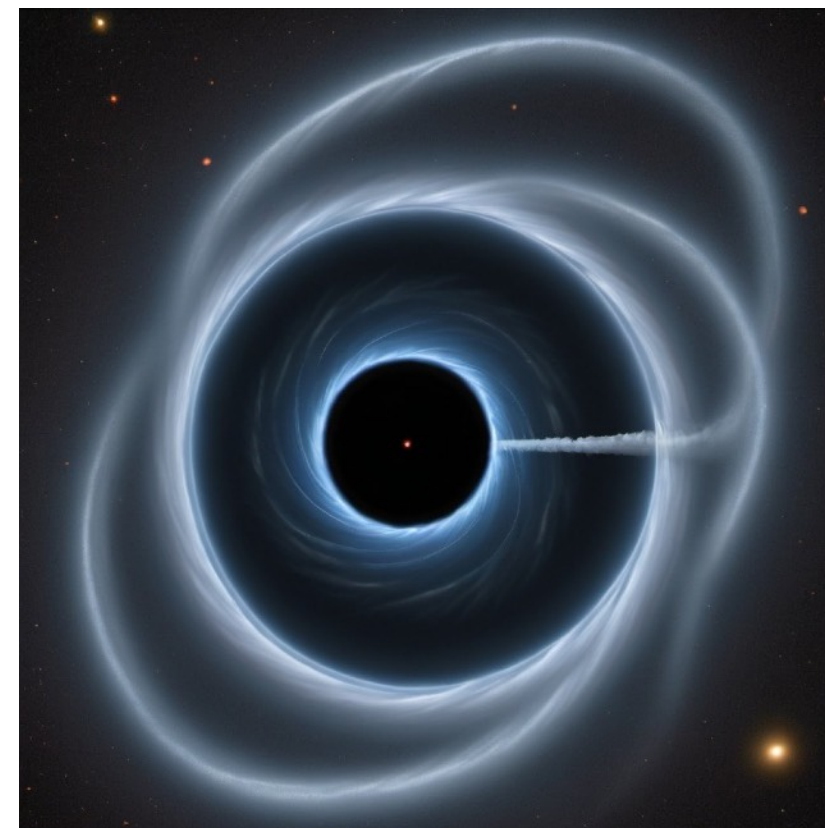
Vector bosons

$$f_{\text{GW}} \approx 645 \text{ Hz} \left(\frac{10 M_{\odot}}{M_{\text{BH}}} \right) \left(\frac{\alpha}{0.1} \right) \text{ (at 1st order)}$$

$$\dot{f} \approx 3 \times 10^{-14} \text{ Hz/s} \left(\frac{10 M_{\odot}}{M_{\text{BH}}} \right)^2 \left(\frac{\alpha}{0.1} \right)^{19} \chi_i^2$$

$$\dot{f} \approx 1 \times 10^{-6} \text{ Hz/s} \left(\frac{10 M_{\odot}}{M_{\text{BH}}} \right)^2 \left(\frac{\alpha}{0.1} \right)^{15} \chi_i^2$$

weak signals that are longer-lived



loud signals that are shorter-lived

grangian [25, 26]. In this paper, we consider linear interaction terms with the electron rest mass m_e and the electromagnetic field tensor $F_{\mu\nu}$:

$$\mathcal{L}_{\text{int}} \supset \frac{\phi}{\Lambda_\gamma} \frac{F_{\mu\nu} F^{\mu\nu}}{4} - \frac{\phi}{\Lambda_e} m_e \bar{\psi}_e \psi_e, \quad (2)$$

where ψ_e , $\bar{\psi}_e$ are the SM electron field and its Dirac conjugate, and Λ_γ , Λ_e parameterise the coupling. Specific types of scalar DM, such as the hypothetical Moduli and Dilaton fields motivated by string theory, have couplings to the QCD part of the SM as well [27–29].

The addition of the terms in Eq. 2 to the SM Lagrangian entails changes of the fine structure constant α and the electron rest mass m_e [2, 3]. The apparent variation of these fundamental constants in turn changes the lattice spacing and electronic modes of a solid, driving changes of its size l and refractive index n :

$$\frac{\delta l}{l} = - \left(\frac{\delta \alpha}{\alpha} + \frac{\delta m_e}{m_e} \right), \quad (3)$$

$$\frac{\delta n}{n} = -5 \cdot 10^{-3} \left(2 \frac{\delta \alpha}{\alpha} + \frac{\delta m_e}{m_e} \right), \quad (4)$$

In this work, we consider a ultralight vector dark matter field $A_\mu(t, x)$, which is regarded as a gauge boson of $U(1)_D$ gauge symmetry with D being a label for a charge, such as B and $B - L$. We assume it interacts with ordinary matter through the coupling to the $U(1)_D$ current J_D^μ . The Lagrangian density \mathcal{L} is then given as

$$\mathcal{L} = -\frac{\varepsilon_0 c^2}{4} F^{\mu\nu} F_{\mu\nu} + \frac{\varepsilon_0}{2} \left(\frac{m_A c^2}{\hbar} \right)^2 A^\mu A_\mu - \epsilon_D e J_D^\mu A_\mu, \quad (1)$$

where $F_{\mu\nu} = \partial_\mu A_\nu - \partial_\nu A_\mu$ is the field strength, c is the speed of light, \hbar is the reduced Planck constant, m_A is the mass of the vector field, ε_0 is the permittivity of vacuum and ϵ_D is the gauge coupling constant normalized by the electromagnetic coupling constant. Since the temporal component of the vector field A_0 is negligibly small, we consider only its spatial components $\vec{A} = (A_x, A_y, A_z)$ in the following discussion.

Isi+ PRD 99, 084042 (2019)

M_i [M_\odot]	χ_i	μ [10^{-13} eV]	α_i	f [Hz]	h_0 [5 Mpc/ r]	τ_{inst} [day]	τ_{GW} [yr]
3	0.90	122	0.273	5.8k	4×10^{-26}	0.1	2
10	0.90	36	0.273	1.7k	1×10^{-25}	0.3	6
60	0.70	4.0	0.179	191	5×10^{-26}	39	8k
60	0.90	6.0	0.273	290	7×10^{-25}	2	38
200	0.85	1.6	0.243	77	1×10^{-24}	12	511
300	0.95	1.4	0.311	66	8×10^{-24}	4	40